Response to reviewer #2
(Reviewer #1 has accepted the manuscript)

The author's response has provided clarification, and the changes to the paper have largely helped to convey better the objectives of the study and the reasoning behind the analysis techniques used. Ideally, I would still recommend measuring the reconnection-driven ionospheric flows at the OCB if the data allow, as this is the most direct method of remotely-sensing reconnection (and its extent) from the ionosphere. However, I do accept that (in the absence of good measurements at the OCB) there is still merit to measuring the extent of reconnection bursts from strong ionospheric flows poleward of the OCB, as is the case here. This has been used in many previous studies, even though it represents a simplified approach. However, the authors still need to consider seriously the points made below before the paper is published.

We thank the reviewer for the positive response and have further improved the manuscript according to the reviewer's useful suggestions. The methodology is updated such that the extent of the flow is measured at 1° (as opposed to 2° used previously) poleward of the OCB. We have further added the extent of the reconnection electric field, which is measured right at the OCB, for all events. The two extents (flow & reconnection electric field) show good consistency. We believe that the updated methodology has strengthened the conclusions of the current study.

Major Comments:

(A) Regarding the latitudes chosen to measure the longitudinal extent:

Obviously, the magnetic local time (MLT) extent and width of the flow channel will change as the flow proceeds further into the polar cap. In all three events, the latitude chosen to determine the longitudinal extent (for panels e and f in figures 2 and 4, and e-h in figure 6) is 2 degrees poleward of the estimated location of the OCB. The variation of the magenta lines encompassing the flow in these figures shows that the extent of the reconnection burst flows, and especially their MLT position can change significantly across these 2 degrees.

The authors have strongly defended their decision and provide comments to justify using data at the more poleward latitude, e.g., lines 384-386 – "While this latitude is 2 degrees poleward of the open-closed field line boundary, the shape of the flow did not change much over the 2 degrees displacement and thus still presents the reconnection extent." My response would be, if this statement is true, then why not present the variation at the OCB? Or, at least at a point closer to the OCB. I am not totally convinced, from looking at the data shown, that this statement is necessarily true. If the authors are convinced that the higher latitude (e.g., 80 degrees) is to be used then showing a comparison of the longitudinal extent of the flows (preferably of the poleward component of the SECS flows and not the line-of-sight (LOS) values [see below]) at

78 and 80 degrees (and possibly at other locations in between) is needed to prove the point.

I am still of the opinion that the closer that you can get to actually using the flows at the estimated OCB location, the better.

To incorporate the reviewer's suggestion, we have updated our methodology in the following two aspects. On one hand, we take the measurements 1° (as opposed to 2° used previously) poleward of the OCB to obtain the extent of the flow. The measurements have been smoothed in latitude with a 1° window, following Chisham et al. [2008], to reduce noise and to fill some gaps. On the other hand, we have derived the extent of the reconnection electric field. The derivation is based on the smoothed velocity at the OCB following the method of *Pinnock et al.* [2003], *Freeman et al.* [2007], *Chisham et al.* [2008].

The updated methodology has been applied to all three events. The results show that the two extents agree with each other (see the updated Figures 3g, 5f, and 7f) despite the data gaps in the derived reconnection electric field due to limited echo availability. The description of the methodology and the results have been added at lines 429-479, 533-538, and 643-647 (track-change version).

(B) Regarding the use of LOS flows and the time series of the longitudinal extent:

The time series plots that show the evolution of the extent of the flows are very informative and help to interpret the evolution of each of the events. However, using LOS measurements for this purpose is not a particularly good idea. The beam directions across each radar field-of-view (FOV) vary by ~+/-26 degrees from the central look direction. Hence, comparing LOS measurements from radar beams looking in multiple directions can be seriously misleading.

For example, lines 511-512 – "The velocity at -74 to -30 degrees MLON dropped by 100-200 m/s during 1900-1910 UT, while the velocity at -88 to -74 degrees MLON did not change substantially" – Firstly, in LOS measurements, changes like this can happen just due to slight changes in the direction of the bulk plasma flow relative to the line-of-sight direction. Secondly, these are LOS measurements made by different radars with different look directions. At the join between the measurements from the two radars (between figs 6e and 6f), the look directions of the beams from the two radars differ by more than 90 degrees. Hence, these two radars will measure very different LOS flows at this location. Hence, it is difficult to match together the two figures, and it should not be attempted! It would be much better to show the temporal evolution of the poleward component of the SECS flow here.

In addition, MLON should not be used as one of the axes in these plots. Variations should be plotted against magnetic local time (MLT). This removes changes in the longitude of the flow that are related solely to the rotation of the Earth, which is not relevant to this study.

Hence, my recommendation is that panel e in figs 2, 4, and 6 would be much clearer, less ambiguous, and more easy to interpret if (i) the poleward component of the SECS flow was plotted instead of the LOS velocity, and (ii) MLT was used on the y-axis instead of MLON.

We have updated the figures following the reviewer's advice. The time series plots in Figures 2e, 5e, and 7e now show the northward component of the 2d SECS flow velocity, which gives a more reliable presentation of flow activity without the ambiguities due to radar looking direction. The evolution pattern has not changed much. This is not surprising to see because we had carefully ensured that the previously used LOS data reflect the major flow velocity component. The y axis of those panels has also been changed to MLT.

(C) Regarding the potential effects of IMF Bx and By on the reconnection burst extent:

I don't think that enough events have been observed to allow there to be any significant comment on the effects of Bx and By on the reconnection burst extent. There is not enough evidence to support the conclusions presented in section 3.4. I would consider removing section 3.4.

We agree that more events should be studied to draw a solid conclusion on solar wind condition dependence. We, however, think that it is useful to present the solar wind conditions and to mention the similarities and differences to the extent we can see within the events studied here. We have moved this section to the discussion section to clarify that we are not counting this section as the results of this paper. We have also toned down the conclusion in the last paragraph of the manuscript for consistency.

Minor Comments:

(1) Lines 82-83 – Petrinec and Fuselier (2003) appears twice in this list of references.
Deleted one.

(2) Line 116 – "FTEs have been observed to be > or < 2 Re wide in local time" – surely this relates to any size of FTE, it will either be smaller or greater than 2 Re. Hence, I don't get the point of this statement.
Changed to "FTEs have been observed to be on the order of a few Re wide in local time"

(3) Line 198 – Remove 'are' after the [Broll et al. 2017] reference.

Removed.

(4) Lines 327-328 – The phrase "…was confined within the utilized few radar FOVs" would be better written as "…was confined within the FOVs of the radars used".
Corrected

(5) Line 553 and Figure 7 – Figure 7 would benefit from the addition of the IMF clock angle variation. The predicted locations of anti-parallel reconnection vary significantly with clock angle, and it is easier to be able to see the clock angle variation without having to visualise the variation based on the variations in IMF By and Bz.
Added. The relative magnitudes of the clock angle is ordered in the same way as the By component.

(6) Lines 569-570 – "Studies have found that small |By|/|Bz| relates to anti-parallel and large |By|/|Bz| to component reconnection" – Significant anti-parallel reconnection still occurs for large |By|/|Bz|, but it occurs at higher latitudes on the magnetopause, away from the equatorial plane
We have changed the statement to "Studies have found that at dayside low latitude magnetopause, small |By|/|Bz| relates to anti-parallel and large |By|/|Bz| to component reconnection".
.

Response to reviewer #3

As stated by the title, the goal of this study is to measure the local time extent of magnetopause reconnection bursts using space-ground coordination. This is a very worthwhile scientific goal because knowing the extent of reconnection is important for understanding the geometrical and other factors influencing the reconnection process, which in turn is fundamental to understanding so much of magnetosphere-ionosphere physics and space weather. However, in my opinion, the definition of a reconnection burst and the methodology used to estimate its extent remains too imprecise and inconsistent that the quoted extents of 3, 5, and 11 Re are of questionable scientific value. If this could be improved then I think this would become an excellent and valuable study.

There are really too many detailed points for me to go through so I shall focus on my major concerns:

1. Definition of a reconnection burst. In their response to my first review, the authors say that they are not interested in the extent of non-zero reconnection rate along the magnetic separator but rather the extent of reconnection bursts within it. However, I can find nowhere in the manuscript where a reconnection burst is objectively defined. The implication seems to be that it is a patch of los or poleward component of ionospheric flow above some threshold that is physically distinct from lower los or poleward flow. In practice, a reconnection burst is effectively defined in the paper as a continuous region with los or poleward flow component exceeding half of the peak value. Thus I see no evidence that a reconnection burst is a distinct physical phenomena but merely the highest reconnection rate region of a more extended reconnecting region.

In view of this, I strongly recommend that you do not use the term burst. Instead in the title and elsewhere you should say that you are measuring the local time extent of magnetopause reconnection (not local time extent of magnetopause reconnection bursts) and then clearly state what your definition of local time extent is. At minimum, this could be the definition that you have been using – the region exceeding half the peak reconnection rate value. However, note that for the a Gaussian spatial variation in reconnection rate (e.g., line 387), the FWHM points are at +/-1.18 standard deviations from the peak and thus about 30% of the total reconnection rate lies outside these bounds.

We agree that "burst" may not the best term. This paper focuses on plasma flows produced by reconnection, i.e., reconnection jets, and our previous manuscript implicitly assumed that reconnection jet extent equates the reconnection extent. Reconnection jets correspond to regions of fast generation of open magnetic flux, and as the reviewer suggested, regions of strong reconnection electric field. We admit that weak reconnection may extend over a broader area, but it is the strong reconnection that effectively contributes to the momentum and energy flow within the magnetosphere. This study explores how wide the strong reconnection electric field is. We have now clarified the motivation in the first introduction paragraph as

"However, reconnection does not occur uniformly across this configuration but has spatial variations [Pinnock et al., 2003; Chisham et al., 2008], and it is the reconnection of high reconnection rates that effectively contributes to the momentum and energy flow within the magnetosphere. Reconnection of high reconnection rates is expected to cause rapid magnetic flux generation and fast reconnection jets. This paper therefore investigates the spatial extent of reconnection through the extents of reconnection jets."

Terminology changes suggested by the reviewer have been made throughout the text. And the definition of reconnection jets has been clarified in the methodology section.

We understand the reviewer's concern that weak reconnection can extend outside the FWHM, and thus now we also mention the 1-sigma extent for a reference (see the response to the comment below). Here we would like to further clarify our reasoning of using FWHM.

While thresholds for ionosphere flow characterization (half maximum, 1/e or 1 sigma) can seem arbitrary, our choice of half maximum is made for the purpose of a consistency with the definition used for reconnection researches in the magnetosphere. In simulations, Shay et al. [2003] measured the reconnection extent as regions of electron speed above half of the peak electron flow speed during reconnection. In in-situ observations, reconnection jets are defined as regions where the plasma velocity quantitatively agrees (>50%) with the Walen relation. Weaker jets could spread over wider regions along the magnetopause but they are not called reconnection jets. Our case study #1 shows that fast poleward ionospheric flows agree with the Walen relation while slow ionospheric flows do not, which gives the physical distinction between fast and slow ionospheric flows. If a lower threshold (e.g., 1/e or 1 sigma) is used, the width determined by the ionosphere flows may become inconsistent with the magnetosphere observations and/or other past studies. We have added one paragraph addressing the definition of width and its relevant limitations in the methodology section as

"As seen in our observations presented below, the longitudinal profile of the fast anti-sunward ionospheric flows has a near bell shaped curve. We measure the extent based on full width at half maximum (FWHM) of the profile at 1° poleward of the open-closed field line boundary. This choice of FWHM is analogous to Shay et al. [2003], where the reconnection extent is measured as regions of electron speed above half of the peak electron flow speed during reconnection. The choice is also supported by magnetopause observations, where we find that ionospheric flows with a speed above half of the peak flow speed map to jets consistent with the Walen relation, while those with a speed below map to jets much slower than the Walen relation (Section 3.1). <u>However, it should be noted that the magnitude of the widths is always dependent on the threshold used, and that half maximum is very likely not the only sensible threshold. Using FWHM excludes ionospheric flows with a speed below half of the peak flow speed. Those flows,</u>

if related to reconnection, associate with comparatively slow generation of open magnetic flux and low contribution to geomagnetic activity."

We have also explicitly stated that the measured widths are FWHM in the abstract and conclusion sections.

Another advantage of FWHM is that the Gaussian slope at half maximum is steeper than that for 1/e or 1 sigma, and thus the extent is less subject to measurement errors (1-2 beam width uncertainty as opposed to several beam width for lower thresholds).

Thus, personally, I think it would be helpful to also quote the full width of non-zero reconnection rate. The full width of non-zero reconnection rate is arguably a better measure too because choosing the half-maximum rather than some other fraction (e.g., 1/e) is arbitrary (see point 3 below) whereas non-zero is not, and the relationship of the FWHM to the total reconnection rate contained within it depends on the shape of the reconnection rate spatial variation. That is, I recommend quoting the region over which the reconnection rate exceeds zero within uncertainties (i.e., the difference from zero is statistically significant). If the non-zero region extends beyond the observed region then the quoted value would be a lower bound.

We have derived the distribution of reconnection electric field for all three events (see Figures 3, 5f, and 7f), based on which we estimate the non-zero reconnection extent.

For case study #1, we added that

"As shown in Figure 3g, the profile of the reconnection electric field had a peak in the azimuthal direction with a limited FWHM, and the FWHM is essentially the same as the flow width just poleward of the boundary (difference being less than the radar spatial resolution). This confirms that our measure of the reconnection jet extent is related to the extent of reconnection of high reconnection rates. Regions of high reconnection rates are localized, although those of low reconnection rate (>0 mV/m) can extend over a much broader region. For example, the western boundary of non-zero reconnection rates was located just at the edge of INV FOV (considering the 15 mV/m uncertainty), and the eastern edge extended beyond INV FOV, likely into where the post-noon flow was originated from. A lower estimate of non-zero reconnection rates is therefore ~4 h MLT. It is likely that there were two components of reconnection at different scales: broad and low-rate background reconnection, and embedded high-rate reconnection."

For case study #2, we added that

"While the reconnection electric field had data gaps due to the limited coverage and backscatter availability at near range gate, it implies a western boundary of FWHM consistent with the flow slightly poleward of it. This is also the western boundary of non-zero reconnection rates considering the 15-mV/m uncertainty. The eastern boundary extended beyond RKN FOV."

For case study #3, we added that

"The reconnection electric field had a similar FWHM to the flow although regions of non-zero reconnection rates again extended beyond the available coverage indicating an overall extent >4 h MLT."

2. Estimation of the reconnection rate. In my previous review, I recommended that the authors estimate the reconnection rate from the ionospheric electric field in the frame of the generally moving open-closed field line boundary, following the methodology of Chisham et al. (2008). I thank the authors for trying this for the Feb 2013 event. However, the authors relegate this to the supporting information and dismiss this approach in lines 393-401 of the main manuscript and in their response. I really must take issue with the reasoning for this and strongly recommend that the Chisham et al method is used:

Firstly, in the authors' response, they reject the need for the method because they say "our approach is consistent with a number of past works cited above", by which I assume that they mean the 17 references from Goertz et al (1985) through Zhang et al. (2008) that they cite in response to my point 1. However, it should be noted that these works are all 10 or more years old and pre-date the Chisham et al. (2008) method. Thus in my view the state of the art has changed since then and this should be reflected in the standard of data analysis used in this paper.

Secondly, the authors argue that the uncertainty in the estimation of the OCB velocity is large and thus it is reasonable to focus "on the velocity profile poleward of the open-closed field line boundary, which is less affected by the error associated with the boundary". So what the authors are effectively saying is that in some way the los velocity several degrees poleward of the OCB is a better estimate of the magnetopause reconnection rate than estimating the electric field in the moving frame of the OCB. How can this be? No scientifically based arguments are given as to why this should be so. I fear that what the authors are really saying is that they don't want to acknowledge and deal with the inconvenience of observational uncertainties when estimating the local time extent of reconnection (whether a burst or not). In my opinion this is not good science.

If one truly wants to estimate the local time of reconnection then one must be able to identify where the reconnection rate is non-zero. This inevitably requires identifying the OCB, its motion, and the ExB velocity component perpendicular to the OCB. As the authors correctly say, first order spatial differences of the OCB latitude from SuperDARN measurements introduce an uncertainty of 45 km in 2 min, corresponding to an OCB velocity uncertainty of 375 m/s or about 23 mV/m. However this can effectively be reduced somewhat using higher-order differences for the time derivative, or considering a longer sampling interval if this seems appropriate. Either way, this uncertainty has to be taken into account, as detailed in Chisham et al. (2008).

Applying the first-order uncertainty to Figure S3 one would conclude that the -83 to -94 MLON region has a non-zero reconnection rate at the 1 sigma level and this is thus the minimum extent of reconnection. Admittedly the 1 sigma level is not very compelling to a statistician but that is the reality and the scientific method. At least you have quantified the extent for a given confidence level even if that level is low.

The alternative is that one limits oneself to determining the extent of high-speed or non-zero los or poleward flows at given latitude, as you have done, but then one cannot really claim that this is the extent of reconnection in my view.

We thank the reviewer for the discussion. We agree that reconnection electric field is important and that it gives a crucial context for interpreting the flow extent. Therefore the calculation of reconnection electric field has now been conducted for all three events and the results are presented in the main body of the paper. The distribution of the reconnection electric field is very similar to the flow, although there are large data gaps in the reconnection electric field due to limited coverage and backscatter at near range gates around the OCB.

If one is to measure the total extent of reconnection including that of low reconnection rate, the extent is larger than our radar FOV. Our radar FOV size serves as a lower estimate of the overall extent (see our response above). This is acknowledged in the text at lines 472-479, 535-538, and 645-647 (track-change version).

3. Patchy versus extended reconnection. To further emphasise what I believe is the questionable scientific value of the three quoted reconnection extents, I would like to compare the los and SECS velocity profiles shown in figures 2f and 6g. The former is inferred to have a reconnection extent of 13 deg MLON or 3 Re at the magnetopause and the latter 63 deg MLON or 11 Re. Yet I suspect from what I can see in figures 2a and 2b that if the velocity profile shown in figure 2f were extended over the full longitudinal extent of the SuperDARN measurements then it would be similar to that in figure 6g.

Specifically figure 6g has a los velocity maximum at -73 deg MLON. It is clearly above the half-maximum value over a 20 deg MLON region between -87 and -65 deg MLON, at or below the half-maximum value between -55 and -65 MLON and rises again to intermediate values between -65 and -20 deg MLON. (Incidentally -27 MLON shown by the black dotted vertical guideline is not the FWHM point). This is concluded to be an extended reconnection example. Figure 2f has a los velocity maximum at -82 deg MLON and is clearly above the half-maximum value over a 13 deg MLON region -92 and -79 deg MLON before dipping down to just below the half-maximum and likely increasing again above it over an extended region beyond the limit of the plot at -70 deg MLON. This is concluded to be a patchy reconnection example yet I believe the distinction between this and the extended reconnection example depends on a marginal difference in the dip below the half-maximum value in the two cases.

For example, if one had chosen 40% of the maximum rather than 50% then both might have been extended. Or if one chose a slightly lower latitude (closer to the OCB) then I suspect from figure 2b that the dip below the half-maximum in Figure 2f might not be as evident. If there is such a sensitivity in the 'reconnection' extent to the velocity threshold and/or latitude then this casts doubt on the scientific robustness and value of the quoted extents, even without the caveats of point 2 above. Apologies if I am wrong but I'd appreciate seeing los and SECS profiles at different latitudes and over the full MLON range to clear this up. Thanks.

We have expanded the longitudinal/MLT range for this event in Figure 2e. Note that the time series plot now shows the northward component of the 2d SECS velocities, which does not have the ambiguities due to radar looking direction. The measurements are also taken from 1° poleward of the OCB as opposed to 2° used previously. We further present the longitudinal cut of this time series plot around the conjunction time (2135 UT) below. The X axis is the distance from magnetic noon. It can be seen that the two flows were separated by an area of low velocity much below the half maximum. The lowest speed between the two flows was ~10 m/s, only 1-2% of the speed at the peak. This is highly contrasted from the broad extent of the flow in Figure 7f.

We would also like to point out there are other features supporting our differentiation of the two flows. Firstly, as seen in Figures 2a-c, the pre- and post-noon flows became more and more separated and propagate towards more and more different directions as they move away from the cusp. This implies that the two flows are driven by different magnetic tension forces. Hence the velocity dip is not a random velocity fluctuation but really distinguishes reconnection associated with different magnetic field topologies. Secondly, the two flows evolved differently in time. The pre-noon flow persisted for ~30 min while the post-noon flow had a ~10-min lifetime. This implies that the two regions of reconnection have quite different spatial and temporal characteristics, and this is the merit of looking beyond the reconnection electric field distribution.

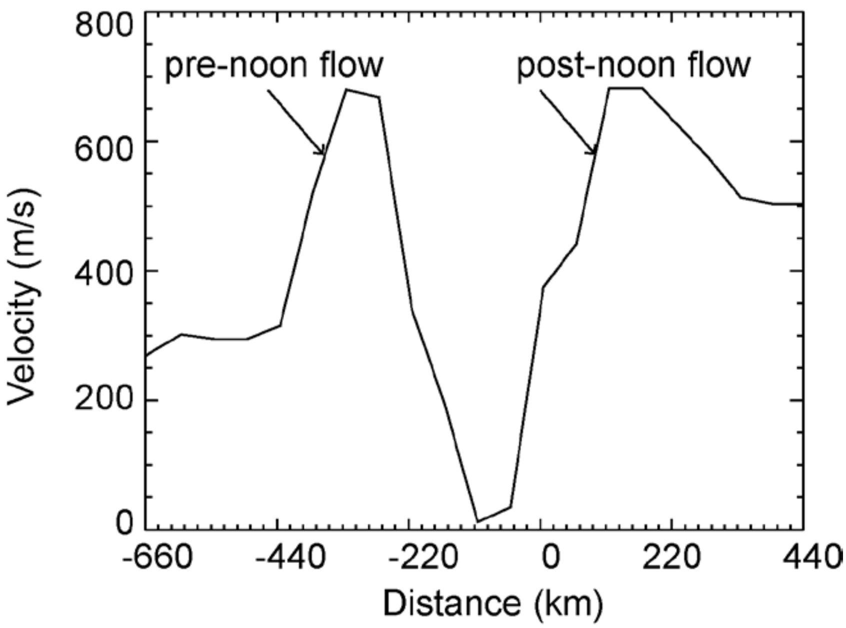

The above clarification has been added to lines 333-340.

4. Other points. Besides the above major points, I'd also like to mention:
a. It's really difficult to relate the MLON profiles with the FOV maps when you don't put MLON labels on the maps!
We have changed the y axis of Figures 2, 5, 7 to MLT to help readers relate to the 2-D snapshots.

b. I think you might be getting your east and west the wrong way round in some places, such as lines 362-366. You say the eastern boundary is at -82 deg MLON and the western boundary is at -77 deg MLON. But isn't westward in the sense of more negative MLON? As confirmed by THA being westward of THE in Figure 1 and Figure 2e.
Corrected.

c. I felt that the argument involving distinguishing between 200 m/s and 220 m/s spectral widths in lines 334-345 to be doubtful. Firstly, I'm not aware that a simple spectral width threshold corresponding to newly-reconnected field line precipitation has been calibrated (as opposed to the Chisham spectral width boundary method). Secondly, the eastward edge of the pre-noon flow region marked by the magenta line in Figure 2a actually lies through the eastern one of the two dark red spectral width regions in Figure 2d, whereas by your argument shouldn't it lie between them or at the eastern edge of the western dark red region? I think this further supports my argument in point 3 above that this is an extended rather than patchy reconnection region.
The purpose is to point out that there may exist additional structures in the broadly enhanced spectral width area. We have toned down the statement as "*there might exist two dark red regions embedded within the ~200-m/s spectral widths. These two regions*

had slightly higher spectral widths than the surrounding (by 20-50 m/s) and possibly corresponded to the two flows".

It actually is not surprising for us to see that the spectral width and the flow did not match exactly. The spectral width is affected by precipitation of electrons and the flow velocity is associated with electric field established by Alfven waves. The two processes are closely related but may not necessarily occur at the exact same instance or location. For the specific event, the region of elevated spectral width seems to be overall displaced to the west of the flow. However, it is also possible that the spatial smoothing of spectral width data (as necessary in inferring the open-closed field line boundary) has contributed to the displacement. This is nevertheless beyond the focus of this study.

d. Why do you not publish all 6 events that you have identified? For example in the supporting information at least as a brief description and summary figure like figure 2f, 4f, 6g for each case. It might help strengthen your conclusions.

We appreciate the reviewer's suggestion but our conclusions are solely based on the three presented events. These events have the clearest, and probably the simplest, flow structures and best space-ground conjunctions. They therefore provide the most convincing evidence among the database. On the other hand, the rest of the events have comparatively small coverage of the flow structures or the reconnection electric field, where an extent cannot be easily obtained. Since those events nevertheless have little relevance to our conclusion, we concern that including them would only distract readers from the main points especially when the paper is already long. We would like to withdraw the statement and only focus on the three presented events.

Local time extent of magnetopause reconnection ~~bursts~~ using space-ground coordination

Ying Zou[1,2], Brian M. Walsh[3], Yukitoshi Nishimura[4,5], Vassilis Angelopoulos[6], J. Michael Ruohoniemi[7], Kathryn A. McWilliams[8], Nozomu Nishitani[9]

1. Department of Astronomy and Center for Space Physics, Boston University, Massachusetts, USA
2. Cooperative Programs for the Advancement of Earth System Science, University Corporation for Atmospheric Research, Boulder, Colorado, USA
3. Department of Mechanical Engineering and Center for Space Physics, Boston University, Boston, Massachusetts, USA
4. Department of Electrical and Computer Engineering and Center for Space Sciences, Boston University, Boston, Massachusetts, USA
5. Department of Atmospheric and Oceanic Sciences, University of California, Los Angeles, California, USA
6. Department of Earth, Planetary and Space Sciences, University of California, Los Angeles, California, USA
7. The Bradley Department of Electrical and Computer Engineering, Virginia Tech, Blacksburg, Virginia, USA
8. Institute of Space and Atmospheric Studies, University of Saskatchewan, Saskatoon, Saskatchewan, Canada
9. Center for International Collaborative Research, Institute for Space-Earth Environmental Research, Nagoya University, Nagoya, Japan

Corresponding author: Ying Zou

1. Department of Astronomy and Center for Space Physics, Boston University, Massachusetts, USA

2. Cooperative Programs for the Advancement of Earth System Science, University Corporation for Atmospheric Research, Boulder, Colorado, USA

yingzou@bu.edu

Keyword: 2784 Solar wind–magnetosphere interactions; 2724 Magnetopause, cusp, and boundary layers; 7835 Magnetic reconnection

Abstract

Magnetic reconnection ~~bursts~~ can vary considerably in spatial extents. At the Earth's magnetopause, the extent generally corresponds to the extent in local time. The extent has been probed by multi-spacecraft crossing the magnetopause, but the estimates have large uncertainties because of the assumption of spatially continuous reconnection activity between spacecraft and the lack of information beyond areas of spacecraft coverage. The limitations can be overcome by using radars examining ionospheric flows moving anti-sunward across the open-closed field line boundary. We therefore infer the extents of reconnection ~~bursts~~ using coordinated observations of multi-spacecraft and radars for three conjunction events. We find that when reconnection jets ~~is active~~occur at only one spacecraft, only the ionosphere conjugate to this spacecraft shows a channel of fast anti-sunward flow. When reconnection ~~is active~~jets occur at two spacecraft and the spacecraft are separated by <1 Re, the ionosphere conjugate to both spacecraft shows a channel of fast anti-sunward flow. The consistency allows us to determine the reconnection ~~burst~~ jet extent by measuring the ionospheric flows. The full-width-at-half-maximum flow extent is ~~260~~200, ~~572~~432, and ~~1260~~ 1320 km, corresponding to a reconnection ~~burst~~ jet extent of ~~3~~2, ~~5~~4, and 11 Re. Considering that reconnection jets emanate from reconnection of a high reconnection rate, the result ~~This strongly~~ indicates that both spatially patchy (a few Re) and spatially continuous and extended reconnection (>10 Re) are possible forms of active reconnection at the magnetopause. Interestingly, the extended reconnection develops from a localized patch via spreading across local time. Potential effects of IMF Bx and By on the reconnection ~~burst~~ extent are discussed.

1. Introduction

A long-standing question in magnetic reconnection is what is the spatial extent of reconnection in the direction normal to the reconnection plane. At the Earth's magnetopause, for a purely southward IMF, this corresponds to the extent in the local time or azimuthal direction. The extent of reconnection has significant relevance to solar wind-magnetosphere coupling, as it controls the amount of energy being passed through the boundary from the solar wind into the magnetosphere and ionosphere. Magnetopause reconnection tends to occur at sites of strictly anti-parallel magnetic fields as anti-parallel reconnection [e.g. *Crooker,* 1979; *Luhmann et al.*, 1984], or occur along a line passing through the subsolar region as component reconnection [e.g. *Sonnerup*, 1974; *Gonzalez and Mozer*, 1974]. Evidence shows either or both can occur at the magnetopause, and the overall reconnection extent can span from a few to 40 Re [*Paschmann et al.*, 1986; *Gosling et al.*, 1990; *Phan and Paschmann*, 1996; *Coleman et al.*, 2001; *Phan et al.*, 2001, 2003; *Chisham et al.*, 2002, 2004, 2008; *Petrinec and Fuselier*, 2003; *Fuselier et al.*, 2002, 2003, 2005, 2010; ~~*Petrinec and Fuselier*, 2003;~~ *Pinnock et al.*, 2003; *Bobra et al.*, 2004; *Trattner et al.*, 2004, 2007, 2008, 2017; *Trenchi et al.*, 2008]. However, reconnection does not occur uniformly across this configuration but has spatial variations [*Pinnock et al.*, 2003; *Chisham et al.*, 2008], and it is the reconnection of high reconnection rates that effectively contributes to the momentum and energy flow within the magnetosphere. Reconnection of high reconnection rates is expected to cause rapid magnetic flux generation and fast reconnection jets. This paper therefore investigates the spatial extent of reconnection through the extents of reconnection jets~~The local time extent of reconnection bursts is the focus of this study~~.

Numerical models show that reconnection ~~bursts~~ tends to occur at magnetic separators, i.e. at the junction between regions of different magnetic field topologies, and global MHD models have identified a spatially continuous separator along the magnetopause [*Dorelli et al.*, 2007; *Laitinen et al.*, 2006, 2007; *Haynes and Parnell*, 2010; *Komar et al.*, 2013; *Glocer et al.*, 2016]. However, little is known about where and over what range along the separators reconnection ~~is active~~proceeds at a high rate. Reconnection in numerical simulations can be activated by introducing perturbations of the magnetic field or can grow spontaneously with instability or resistivity inherent in the system [e.g. *Hesse et al.*, 2001; *Scholer et al.*, 2003]. When reconnection develops as patches (as due to the instabilities or localized perturbations), the patches can spread in the direction out of the reconnection plane [*Huba and Rudakov,* 2002; *Shay et al.* 2003; *Lapenta et al.*, 2006; *Nakamura et al.*, 2012; *Shepherd and Cassak*, 2012; *Jain et al.*, 2013]. The patches either remain patchy after spreading if the current layer is thick, or form an extended X-line if the current layer is already thin [*Shay et al.*, 2003].

Studies have attempted to constrain the extent of reconnection ~~bursts~~ based on fortuitous satellite conjunctions where the satellites detect reconnection jets ~~signatures of active reconnection~~ at the magnetopause at different local times nearly simultaneously [*Phan et al.*, 2000, 2006; *Walsh et al.*, 2014a, 2014b, 2017]. The satellites were separated by a few Re in *Phan et al.* [2000] and *Walsh et al.* [2014a, 2014b, 2017], and >10 Re in *Phan et al.* [2006], and this is interpreted as the reconnection being active over ~~wider than~~ a few Re and even 10 Re, respectively. At the magnetopause, reconnection ~~bursts~~ of a few Re ~~are~~ is often referred to as spatially patchy [e.g., *Fear et al.*, 2008, 2010], and reconnection ~~bursts~~ of >10 Re ~~are~~ is spatially extended [*Dunlop et al.*, 2011; *Hasegawa et al.*, 2016]. The term patchy has also been used to describe the temporal characteristics of reconnection [e.g. *Newell and Meng,* 1991]. But this paper primarily focuses on the spatial properties. The extent ~~of reconnection bursts~~ has been alternatively determined by studying the structures of newly reconnected flux tubes, i.e., flux transfer events (FTEs) [*Russell and Elphic*, 1978; *Haerendel et al.*, 1978]. Conceptual models regard FTEs either as azimuthally narrow flux tubes that intersect the magnetopause through nearly circular holes, as formed by spatially patchy reconnection [*Russell and Elphic*, 1978], or as azimuthally elongated bulge structures or flux ropes that extend along the magnetopause, as formed by spatially extended reconnection [*Scholer*, 1988; *Southwood et al.*, 1987; *Lee and Fu*, 1985]. FTEs have been observed to ~~be > or <2 Re~~be on the order of a few Re wide ~~wide~~ in local time [*Fear et al.*, 2008, 2010; *Wang et al.*, 2005, 2007]. FTEs have ~~even~~ also been observed across ~20 Re from the subsolar region to the flanks [*Dunlop et al.*, 2011]. But it is unclear whether these FTEs are branches of one extended bulge or flux rope, or multiple narrow tubes formed simultaneously. When the satellites are widely spaced, it is in general questionable whether a reconnection ~~burst~~jet/FTE is spatially continuous between the satellites or whether satellites detect the same moving reconnection ~~burst~~jet/FTE. Satellites with a small separation may possibly measure the same reconnection ~~burst~~jet/FTE, but only provide a lower limit estimate of the extent. A reconnection ~~burst~~jet/FTE may also propagate or spread between satellite detection but satellite measurements cannot differentiate the spatial and temporal effects.

This situation can be improved by studying ionospheric signatures of reconnection ~~bursts~~ and FTEs, since their spatial sizes in the ionosphere can be obtained from wide field ground instruments or Low-Earth orbit spacecraft. The ionospheric signatures include poleward moving auroral forms (PMAFs), channels of flows moving anti-sunward across the open-closed field line boundary [e.g., *Southwood*, 1985], and cusp precipitation [*Lockwood and Smith*, 1989, 1994; *Smith et al.*, 1992]. Radar studies have shown that the flows can differ considerably in size, varying from tens of km [*Oksavik et al.*, 2004, 2005], to hundreds of km [*Goertz et al.*, 1985; *Pinnock et al.*, 1993, 1995; *Provan and Yeoman*, 1999; *Thorolfsson et al.*, 2000; *McWilliams et al.*, 2001a, 2001b], and to thousands of km [*Provan et al.*, 1998; *Nishitani et al.*, 1999; *Provan and Yeoman*, 1999]. A similarly broad distribution has been found for PMAFs [e.g. *Sandholt et al.*, 1986, 1990; *Lockwood et al.*, 1989, 1990; *Milan et al.*, 2000, 2016] and the cusp [*Crooker et al.*, 1991; *Newell and Meng*, 1994; *Newell et al.*, 2007]. This range of spatial sizes in the ionosphere approximately corresponds to a range from <1 to >10 Re at the magnetopause. However, care needs to be taken when interpreting the above ionospheric features, since they could also form due to other drivings such as solar wind dynamic pressure pulses [*Lui and Sibeck*, 1991; *Sandholt et al.*, 1994]. An unambiguous proof of their connection to magnetopause reconnection requires simultaneous space-ground coordination [*Elphic et al.*, 1990; *Denig et al.*, 1993; *Neudegg et al.*, 1999, 2000; *Lockwood et al.*. 2001; *Wild et al.*, 2001, 2005, 2007; *McWilliams et al.*, 2004; *Zhang et al.*, 2008].

Therefore a reliable interpretation of reconnection ~~burst~~ extent has been difficult due to observation limitations. We will address this by comparing the extents probed by multi-spacecraft and radars using space-ground coordination. On one hand, this enables us to investigate whether reconnection spans continuously between satellites, and how wide reconnection extends beyond satellites. On the other hand, this helps to determine whether reconnection is the driver of ionospheric disturbances and whether the in-situ extent is consistent with the ionospheric disturbance extent.

~~It may be noteworthy to point out that we only address the reconnection extent in the local time direction, similarly to previous observations. If the reconnection X-line has a tilted orientation relative to the equatorial plane, the local time extent will be shorter than the total extent. How X-lines tilt is a subject of ongoing research. Various models have been proposed to predict the tilt~~

~~[*Alexeev et al.*, 1998; *Moore et al.*, 2002; *Trattner et al.*, 2007; *Swisdak and Drake*, 2007; *Borovsky*, 2013; *Hesse et al.*, 2013] but their performance is still under test [e.g., *Komar et al.*, 2015]. The local time extent affects the amount of magnetic flux opened in the solar wind-magnetopshere coupling [e.g. *Newell et al.*, 2007].~~

2. Methodology

We study the local time extent of reconnection jets as a characteristic extent of reconnection. We use conjugate measurements between the Time History of Events and Macroscale Interactions during Substorms (THEMIS) [*Angelopoulos*, 2008] and Super Dual Auroral Network (SuperDARN) [*Greenwald et al.*, 1995]. We focus on intervals when the IMF in OMNI data remains steadily southward. We require that two of the THEMIS satellites fully cross the magnetopause nearly simultaneously and that the satellite data provide clear evidence for reconnection occurring or not. The full crossings are identified by a reversal of the Bz magnetic field and a change in the ion energy spectra. The requirements of nearly simultaneous crossings and steady IMF conditions help to reduce the spatial-temporal ambiguity by satellite measurements, where the presence/absence of reconnection ~~signatures~~ jets at different local times likely reflects spatial structures of reconnection. Reconnection can still possibly vary between the two satellite crossings, and we use the radar measurements to examine whether the reconnection of interest has continued to exist and maintained its spatial size.

Identification of reconnection jets in the magnetosphere is based on the f~~F~~luid (MHD) evidence of magnetopause reconnection~~ includes plasma bulk flow acceleration at the magnetopause~~. Reconnection accelerates plasma bulk flow to Alfvenic speed producing reconnection jets at the magnetopause, and the~~This~~ acceleration should be consistent with the prediction of tangential stress balance across a rotational discontinuity, i.e. Walen relation [*Hudson*, 1970; *Paschmann et al.*, 1979]. The Walen relation is expressed as

$$\Delta V_{predicted} = \pm(1-\alpha_1)^{1/2}(\mu_o\rho_1)^{-1/2}[B_2(1-\alpha_2)/(1-\alpha_1) - B_1] \qquad (1)$$

Where ΔV is the change in the plasma bulk velocity vector across the discontinuity. B and ρ are the magnetic field vector and plasma mass density. μ_0 is the vacuum permeability. $\alpha = (p_{\parallel} - p_{\perp})\mu_0/B^2$ is the anisotropy factor where $p_{\parallel}$ and $p_{\perp}$ are the plasma pressures parallel and perpendicular to the magnetic field. The magnetic field and plasma moments are obtained from the fluxgate magnetometer (FGM) [*Auster et al.*, 2008] and the ElectroStatic Analyzers (ESA) instrument [*McFadden et al.*, 2008]. The plasma mass density is determined using the ion number density, assuming a mixture of 95% protons and 5% helium. The subscripts 1 and 2 refer to the reference interval in the magnetosheath and to a point within the magnetopause, respectively. The magnetosheath reference interval is a 10-s time period just outside the magnetopause. The point within the magnetopause is taken at the maximum ion velocity change across the magnetopause. We ensure that the plasma density at this point is >20% of the magnetosheath density to avoid the slow-mode expansion fan [*Phan et al.*, 1996]. We compare the observed ion velocity change with the prediction from the Walen relation. The level of agreement is measured by $\Delta V^* = \Delta V_{obs} \cdot \Delta V_{predicted} / |\Delta V_{predicted}|^2$, following *Paschmann et al.* [1986]. Here $\Delta Vobs$ is the observed ion velocity change. By convention only the velocity changes with $\Delta V^* > 0.5$ are classified as reconnection jets [e.g., *Phan et al.*, 1996; 2013].

To further ensure that reconnection occurs, we examine the ~~A~~ kinetic signature of reconnection, which is ~~found as~~ D-shaped ion distributions at the magnetopause. As magnetosheath ions encounter newly opened magnetic field lines at the magnetopause, they either transmit through the magnetopause entering the magnetosphere or reflect at the boundary. The transmitted ions have a cutoff parallel velocity (i.e. de-Hoffman Teller velocity) below which no ions could enter the magnetosphere. The D-shaped ion distributions are deformed into a crescent shape as ions travel away from the reconnection site [Broll et al. 2017]are. We require the satellites to operate in the Fast Survey or Burst mode in which ion distributions are available at 3 s resolution.

We determine reconnection being active if the plasma velocity change across the magnetopause is consistent with the Walen relation with ΔV^{*} >= 0.5, and if the ions at the magnetopause show a D shape distribution. Reconnection is deemed absent if neither of the two signatures is detected. We require that at least one of the two satellites observe reconnection signatures. Reconnection is regarded as ambiguous if only one of the two signatures is detected, and such reconnection is excluded from our analysis.

We mainly use the three SuperDARN radars located at Rankin Inlet (RKN, geomagnetic 72.6° MLAT, -26.4° MLON), Inuvik (INV, 71.5° MLAT, -85.1° MLON), and Clyde River (CLY, 78.8° MLAT, 18.1° MLON) to measure the ionospheric convection near the dayside cusp. The three radars have overlapping field of views (FOVs), enabling a reliable determination of the 2-d convection velocity. The FOVs cover the ionosphere >75° MLAT, covering the typical location of the cusp under weak and modest solar wind driving conditions [i.e., *Newell et al.*, 1989] and the high occurrence region of reconnection-related ionospheric flows [*Provan and Yeoman,* 1999] with high spatial resolution. Data from Saskatoon (SAS, 60° MLAT, -43.8° MLON) and Prince George (PGR, 59.6° MLAT, -64.3° MLON) radars are also used when data are available. The measurements of these two radars at far range gates can overlap with the cusp. The radar data have a time resolution of 1-2 min. We focus on observations ±3 h MLT from magnetic noon (approximately 1600-2200 UT). The satellite footprints should be mapped close to the radar FOVs under the Tsyganenko (T89) model [*Tsyganenko*, 1989]. Footprints mapped using different

Tsyganenko (e.g., T96 or T01 [*Tsyganenko*, 1995, 2002a, 2002b]) models have similar longitudinal locations (difference <100 km), implying the longitudinal uncertainty of mapping to be small. The latitudinal uncertainty can be inferred by referring to the open-closed field line boundary as estimated using the 150 m/s spectral width boundary [e.g., *Baker et al.*, 1995, 1997; *Chisham and Freeman*, 2003]. And T89 has given the smallest latitudinal uncertainty for the studied events. We surveyed years 2014-2016 during the months when the satellite apogee was on the dayside, and ~~found 6 such conjunctions~~present three events in the paper.

The ionospheric signature of reconnection ~~burst~~ jets includes fast anti-sunward flows moving across the open-closed field line boundary. We obtain the flow velocity vectors by merging line-of-sight (LOS) measurements at the radar common FOVs [*Ruohoniemi and Baker*, 1998], and these merged vectors reflect the true ionospheric convection velocity. However, the radar common FOVs are hundreds of km wide only, which can be too small to cover the full azimuthal extent of the reconnection-related flows (which are up to thousands of km wide). We therefore also reconstruct the velocity field using the Spherical Elementary Current Systems (SECS) method [*Amm et al.*, 2010]. Similar to the works by *Ruohoniemi et al.* [1989] and *Bristow et al.* [2016], the SECS method reconstructs a divergence-free flow pattern using all LOS velocity data. We refer to these velocities as SECS velocities. The accuracy of SECS velocities can be validated by comparing to the LOS measurements and the merged vectors. SECS velocities work best in regions with dense echo coverage and those around sparse echoes are not reliable and thus are excluded from our analysis.

The third way of obtaining a velocity field is Spherical Harmonic Fit (SHF). This method uses the LOS measurements and a statistical convection model to fit the distribution of electrostatic potential, which is expressed as a sum of spherical harmonic functions [*Ruohoniemi and Baker*, 1998]. The statistical model employed here is *Cousins and Shepherd* [2010]. While this method may suppress small or meso-scale velocity details, such as, sharp flow gradients or flow vortices, we compare SHF velocities with the LOS measurements and merged vectors to determine how well the SHF velocities depict the velocity details.

As seen in our observations presented below, the longitudinal profile of the fast anti-sunward ionospheric flows has a near bell shaped curve. We measure the extent based on full width at half maximum (FWHM) of the profile at 1° poleward of the open-closed field line boundary. The choice of FWHM is analogous to *Shay et al.* [2003], where the reconnection extent is measured as regions of electron speed above half of the peak electron flow speed during reconnection. The choice is also supported by magnetopause observations, where we find that ionospheric flows with a speed above half of the peak flow speed map to jets consistent with Walen relation, while those with a speed below map to jets much slower than the Walen relation (Section 3.1). However, it should be noted that the magnitude of the widths is always dependent on the threshold used, and that half maximum is very likely not the only sensible threshold. Using FWHM excludes ionospheric flows with a speed below half of the peak flow speed. Those flows, if related to reconnection, associate with comparatively slow generation of open magnetic flux and low contribution to geomagnetic activity.

Among the ~~six~~ three presented events~~-~~,~~we identified, we present three representative conjunction events in Sections 3.1-3.3. T~~ the time separations of magnetopause crossings by two satellites are 1, 2, and 30 min. While the time separation for the third case is somewhat long, we distinguish the spatial and temporal effects using the radar data. Although the three events occurred under similar IMF Bz conditions, the reconnection-related flows in the ionosphere had an azimuthal extent varying from a few hundred km (Sections 3.1-3.2) to more than a thousand km wide (Section 3.3).

This corresponds to reconnection ~~bursts~~ of a few to >10 Re wide indicating that both spatially patchy (a few Re) and spatially continuous and extended reconnection (>10 Re) are possible forms of active reconnection at the magnetopause. Interestingly, the extended reconnection was found to arise from a spatially localized patch that spreads azimuthally. Potential effects of IMF Bx and By on the reconnection ~~burst~~ extent are discussed in Section ~~3.~~4.

Note that reconnection can happen over various spatial and temporal scales and our space-ground approach can resolve reconnection ~~bursts~~ that are larger than 0.5 Re and persist longer than a few minutes. This is limited by the radar spatial and temporal resolution, and the magnetosphere-ionosphere coupling time which is usually 1-2 min [e.g. *Carlson et al.*, 2004]. This constraint is not expected to impair the result because reconnection ~~bursts~~ above this scale ~~have~~ has been found to occur commonly in statistics (see the Introduction section for spatial and *Lockwood and Wild* [1993], *Kuo et al.* [1995], *Fasel* [1995], and *McWilliams et al.* [1999] for temporal characteristics).

3. Observations

3.1. Spatially patchy reconnection active at one satellite only

3.1.1 In-situ satellite measurements

On February 2, 2013, THA and THE made simultaneous measurements of the dayside magnetopause with a 1.9 Re separation in the Y direction around 21:25 UT. The IMF condition is displayed in Figure 1a and the IMF was directed southward. The satellite location in the GSM coordinates is displayed in Figure 1b, and the measurements are presented in Figure 2. The magnetic field and the ion velocity components are displayed in the LMN boundary normal coordinate system, where *L* is along the outflow direction, *M* is along the X-line, and *N* is the current sheet normal. The coordinate system is obtained from the minimum variance analysis of the magnetic field at each magnetopause crossing [*Sonnerup and Cahill*, 1967]. Figures 2g-p show that both satellites passed from the magnetosheath into the magnetosphere, as seen as the sharp changes in the magnetic field, the ion spectra, and the density (shaded in pink).

As THE crossed the magnetopause boundary layer (2122:57-2123:48 UT), it detected ~~both fluid and kinetic signatures of reconnection. It observed~~ a rapid, northward-directed plasma jet within the region where the magnetic field rotated (Figures 2g and 2j). The magnitude of this jet relative to the sheath background flow reached 262 km/s at its peak, which was 72% of the predicted speed of a reconnection jet by the Walen relation (366 km/s, not shown). The angle between the observed and predicted jets was 39°. THE also detected kinetic signatures of reconnection. The ion distributions in Figure 2k showed a distorted D-shaped distribution similar to the finding of by *Broll et al.* [2018]. The distortion is due to particles traveling in the field-aligned direction from the reconnection site to higher magnetic field region, and *Broll et al.* [2018] estimated the traveling distance to be a few Re for the observed level of distortion.

THA crossed the magnetopause one to two minutes later than THD (2124:48-2125:13 UT). While it still identified a plasma jet at the magnetopause (Figures 2l and 2o), the jet speed was significantly smaller than what was predicted for a reconnection jet (80 km/s versus 380 km/s in the *L* direction). The observed jet was directed 71° away from the prediction. The ion distributions deviated from clear D-shaped distributions (Figure 2p). ~~Reconnection was thus much less active at THA local time than at THE.~~ This suggests that the ~~X-line of the active reconnection~~reconnection jet at THE likely did not extend to THA.

3.1.2 Ground radar measurements

The velocity field of the dayside cusp ionosphere during the satellite measurements is shown in

Figures 2a-c. Figure 2a shows the radar LOS measurements at 21:25 UT, as denoted by the color tiles, and the merged vectors, as denoted by the arrows. The colors of the arrows indicate the merged velocity magnitudes, and the colors of the tiles indicate the LOS speeds that direct anti-sunward (those project to the sunward direction appear as black). Fast (red) and anti-sunward flows are the feature of our interest. One such of this flow can be identified in the pre-noon sector, which had a speed of ~800 m/s and was directed poleward and westward. As the merged vector arrows indicate, the velocity vectors have a major component close to the INV beam directions and thus the INV LOS velocities reflect the flow distribution. The flow crossed the open-closed field line boundary, which was located at 78° MLAT based on the spectral width (Figure 2d and S1). This flow thus meets the criteria of being an ionospheric signature of magnetopause reconnection jets~~burst~~. Another channel of fast flow was present in the post-noon sector. This post-noon flow was directed more azimuthally and was increasingly separated from the pre-noon flow as it moved away from the noon (see the ~~by a~~ region of slow velocities at >79° MLAT around noon). The difference in flow trajectories implies that these flows were driven by different magnetic tension forces. They also evolved differently over time as seen in Figure 2e which is discussed below. The ~~two flows are thus two different structures~~ flows thus likely originated~~ing~~ from two reconnection regions that were associated with different magnetic field topologies and different temporal variabilities ~~two spatially discontinuous reconnection bursts~~. Since the satellites were located in the pre-noon sector we focus on the pre-noon flow below.

The flow had a limited azimuthal extent. The extent is determined at half of the maximum flow speed, which was ~400 m/s. Figure 2f discussed below shows a more quantitative estimate of the extent. In Figure 2a, we mark the eastern and western boundaries with the dashed magenta lines, across which the LOS velocities dropped from red to blue/green colors.

Figure 2b shows the SECS velocities, denoted by the arrows. The SECS velocities reasonably reproduced the spatial structure of the flows seen in Figure 2a. The flow boundaries were marked by the dashed magenta lines, across which the flow speed dropped from red to blue. Across the flow western boundary the flow direction also reversed. The equatorward-directed flows are interpreted as the return flow of the poleward flows, as sketched in *Southwood* [1987] and *Oksavik et al.* [2004].

The velocity field reconstructed using the SHF velocities is shown in Figure 2c (obtained through the Radar Software Toolkit (http://superdarn.thayer.dartmouth.edu/software.html)). This is an expanded view of the global convection maps in Figure S2 focusing on the dayside cusp. Comparing Figures 2c and S2 reveals that the employed radars listed in Section 2 have contributed to the majority of the backscatters on the dayside. This is because this event (same for the following two events) occurred under non-storm time, where the open-closed field line was confined within ~~the utilized few radar FOVs~~the FOVs of the radars used. During storm time the boundary expands to lower latitude where backscatter from a wider network of radars may be available. The SHF velocities also captured the occurrence of two flows in the pre- and post-noon sectors, respectively, although the orientation of the flows were ~~less azimuthally-aligned than~~slightly different from Figure 2a or 2b. The difference is likely due to the contribution from the statistical potential distribution under the southward IMF. The flow western and eastern boundaries were again marked by the dashed magenta lines.

Figure 2d shows spectral width measurements. Large spectral widths can be produced by soft (~100 eV) electron precipitation [*Ponomarenko et al.*, 2007], and evidence has shown that the longitudinal extent of large spectral widths correlates with the extent of PMAFs [*Moen et al.*, 2000] and of poleward flows across the open-closed field line boundary [*Pinnock and Rodger*, 2001].

Large spectral widths thus have the potential to reveal the reconnection ~~burst~~ extent. For the specific event under examination, the region of large spectral widths, appearing as red color, spanned from 10.5 to 14.5 h MLT if we count the sporadic scatters in the post-noon sector. This does not contradict the flow width identified above because the wide width reflects the summed width of the pre- and post-noon flows. In fact a more careful examination shows that there might exist two dark red regions (circled in red, the red dashed line is due to the discontinuous backscatters outside the INV FOV) ~~the presence of two dark red (>220 m/s spectral width) regions~~ embedded within the ~200-m/s spectral widths ~~(circled in red, the red dashed line is due to the discontinuous backscatters outside the INV FOV)~~. These two regions had slightly higher spectral widths than the surrounding (by ~20-50 m/s) and possibly~~,~~ corresponded~~ing~~ to the two flows.

Figures 2a-c all observed a channel of fast anti-sunward flow in the pre-noon sector of the high latitude ionosphere, and the flow had a limited azimuthal extent. If the flow corresponded to a magnetopause reconnection jet, the reconnection ~~burst~~ jet is expected to span over a limited local time range. This is consistent with the THEMIS satellite observation in Section 3.1.1, where THE at Y = -2.9 Re detected a clear reconnection ~~signatures~~jet, while THA at Y = -4.8 Re did not. In fact, if we project the satellite location to the ionosphere through field line tracing under the T89 model, THE was positioned at the flow longitude, while THA was to the west of the flow embedded in weak convection (Figure 2a).

While this paper primarily focuses on the spatial extent of reconnection ~~bursts~~, the temporal evolution ~~of reconnection~~ can be obtained from the time series plot in Figure 2e. Figure 2e presents the northward component of the SECS velocity~~INV LOS measurements~~ along ~~80~~79° MLAT (just 1° poleward of the open-closed field line boundary ~~with good LOS measurements~~) as functions of magnetic ~~longitude~~ local time (~~MLON~~MLT) and time. Here we only show the northward component of the SECS velocity as this component represents reconnecting flows across an azimuthally-aligned open-closed field line boundary. Similar to the snapshots, ~~the color represents LOS speeds that project to the anti-sunward direction, and~~ the flow of our interest appears as a region of red color. The time and the location where THA and THE crossed the magnetopause are marked by the crosses~~vertical and horizontal lines~~. The pre-noon flow emerged from a weak background ~~at 2120~~ from 2122 UT and persisted for ~>30 min~~ in INV FOV~~, while the post-noon flow only lasted for ~10 min. Minutes following the onset the pre-noon flow spread in width, where the western boundary of the red color moved from 10.7 to 10.5 h MLT, and the eastern boundary moved to 11.2 to 11.5 h MLT. After 2134 UT the spreading ceased and the entire flow moved westward (the western boundary moved beyond the FOV). ~~At the onset the flow eastern boundary was located at -82° MLON, and interestingly, this boundary spread eastward with time in a similar manner as events studied by Zou et al. [2018]. The flow western boundary was located around -77° MLON during 2120-2134 UT, and started to spread eastward after 2134 UT.~~ Hence the reconnection-related ionospheric flow, once formed, has spread in width and displaced ~~eastward~~westward. The spreading behavior is similar to events studied by Zou et al. [2018], and is interpreted to relate to spreading of the reconnection extent seen in simulation studies (see introduction). The spreading has also been noticed in the other two events (see Section 3.3), indicating that this could be a common development feature of the reconnection-related flows. ~~The spreading was fast in the first 6 min and then slowed down stabilizing at a finite flow extent until the eastern boundary went outside FOV at 2134 UT.~~

A consequence of the flow temporal evolution is that THA, which was previously outside the reconnection-related flow, became immersed in the flow from 2130 UT, while THE, which was previously inside the flow, was left outside from 2142 UT (Figure 2e). This implies that at the magnetopause the reconnection has spread azimuthally sweeping across THA, and has slid in the –y direction away from THE. This is in perfect agreement with satellite measurements shown in Figures 2q-z. Figures 2q-z presents subsequent magnetopause crossings made by THA and THE following the crossings in Figures 2g-p. THA detected an Alfvenic reconnection jet and a clear D-shape ion distribution, and THE detected a jet much slower than the Alfvenic speed and an ion distribution without a clear D-shape. This corroborates the connection between the in-situ reconnection ~~signatures~~ jet with the fast anti-sunward ionospheric flow, and reveals the dynamic evolution of reconnection in the local time direction. On the other hand, this also sheds light on the nature of the slow convection outside the fast flow, which corresponds to sub-Alfvenic jets at the magnetopause.

We quantitatively determine the flow extent in Figure 2f. Figure 2f shows the profile of the northward component of the SECS velocity at 2129 UT ~~the INV LOS velocity profile at 2125 UT~~ as a function of ~~magnetic longitude and~~ the distance from~~-~~ magnetic noon~~0° MLON~~. The 2129 UT is the time when the flow extent has slowed down from spreading and stabilized. The profile should theoretically be taken just poleward of the open-closed field line boundary. In practice we smooth the velocity in latitude with a 1° window and take measurements 1° poleward of the open-closed field line boundary. The profile has a near bell shaped curve, and the FWHM was 200 km at an altitude of 250 km. Also shown is the INV LOS velocity profile, which is obtained in a similar manner as the SECS one. The LOS velocity profile also gives a narrow FWHM, which was 280 km. ~~The 2125 UT is the same time instance as in Figures 2a-c and is the time when the flow extent has slowed down from spreading and stabilized. The profile is taken along 80° MLAT. While this latitude is 2° poleward of the open-closed field line boundary, the shape of the flow did not change much over the 2° displacement and thus still presents the reconnection extent~~. ~~The flow velocity~~

profile has a skewed Gaussian shape, and we quantify the flow extent as the full-width-at-half-maximum (FWHM). The FWHM was 13° in MLON or 260 km at an altitude of 250 km. Also shown is the SECS velocity profile. Here we only show the northward component of the SECS velocity as this component represents reconnecting flows across an azimuthally-aligned open-closed field line boundary. The SECS velocity profile gives a FWHM of 13.5° in MLON or 270 km, very similar to the LOS profile.

While it is commonly assumed that the extent of reconnection jets reflects the extent of reconnection, we test the assumption by calculating the distribution of reconnection electric field in Figure 3. It is noteworthy mentioning that the velocity profile obtained above approximates to the profile of reconnection electric field along the open-closed field line boundary (details in Figure S3). Reconnection electric field can be estimated by measuring the flow across the open-closed field line boundary in the reference frame of the boundary [*Pinnock et al.*, 2003; *Freeman et al.*, 2007; *Chisham et al.*, 2008],] and . we follow this procedure to derive the its distribution across local time. A close-up presentation of the open-closed field line boundary is shown in Figures 3a-c around the space-ground conjunction time and longitude. The open-closed field line boundary, drawn as the dashed black line, is identified following *Chisham and Freeman* [2003, 2004] and *Chisham et al.* [2004b, 2005a, 2005b, 2005c]. The boundary was almost along a constant magnetic latitude. The motion of the boundary is obtained by inspecting the time series of the spectral width measurements along each radar beam and examples are given for INV beams 4, 7, and 10 in Figures 3d-f. Subtracting the speed of the boundary from that of the flow (in the rest frame) across the boundary gives the flow speed in the reference frame of the boundary. Assuming that the flow is E × B drift, electric field can be derived and this is the ionosphere-mapped reconnection electric field. The flow speed across the boundary is taken from the 1°-averaged speed at the boundary latitude (similar to *Chisham et al.* [2008]). Note that a precise determination of the boundary motion could be subject to radar spatial and temporal resolution and the error can be as large as 300 m/s or 15 mV/m.

As shown in Figure 3g, the profile of the reconnection electric field had a peak in the azimuthal direction with a limited FWHM, and the FWHM is essentially the same as the flow width just poleward of the boundary (difference being less than the radar spatial resolution)However, a precise determination of the boundary motion is subject to radar spatial and temporal resolution and for a slow motion like the events studied in this paper (Figure S1), the signal to noise ratio is lower than one. For this reason this paper focuses on the velocity profile poleward of the open-closed field line boundary, which is less affected by the error associated with the boundary. This establishes the relation between our measure of the reconnection jet extent and the extent of reconnection of high reconnection rates. Regions of high reconnection rates are localized, although those of low reconnection rates (>0 mV/m) can extend over a much broader region. For example, the western boundary of non-zero reconnection rates was located just at the edge of INV FOV (considering the 15 mV/m uncertainty), and the eastern edge extended beyond INV FOV, likely into where the post-noon flow was originated from. A lower estimate of the extent of non-zero reconnection rates is therefore ~4 h MLT. It is likely that there were two components of reconnection at different scales: broad and low-rate background reconnection, and embedded high-rate reconnection.

To infer the reconnection burst extent at the magnetopause, we project the flow width extent based on the SECS in the ionosphere to the equatorial plane. The result suggests that the reconnection local time extent was ~23 Re.

Before closing this section, we would like to point out that the determined extent is characterized by the FWHM of the fast anti-sunward ionospheric flow, which allows weak flows to extend beyond the flow extent. When THA and THE were positioned within the weak flows in the ionosphere, they at the magnetopause observed flows much weaker than the Walen prediction. This may imply that there were two components of reconnection at different scales in this event: weak background reconnection signified by the slow flows, and embedded strong reconnection bursts signified by the fast flows.

3.2. Spatially patchy reconnection active at both satellites

3.2.1. In-situ satellite measurements

On April 19, 2015, under a southward IMF (Figure 3a4a), THA and THE crossed the magnetopause nearly simultaneously (<2 min lag) with a 0.5 Re separation in Y (Figure 3b4b). They passed from the magnetosheath into the magnetosphere. Both satellites observed jets in the V_L component at the magnetopause (Figures 4g5g-p). The jet at THA at ~1828:05 UT had a speed of 84% of and an angle within ~15° from the Walen prediction. The jet at THE at ~1826:25 UT had a speed of 95% of and an angle of ~29° from the Walen prediction. The ion distributions at THA and THE exhibit clear D-shaped distributions., Reconnection indicative of active reconnection thus occurred at these twoboth local times.

Section 3.2.2. Ground radar measurements

During the satellite measurements, the radars observed a channel of fast anti-sunward flow around magnetic noon (Figures 4a5a-c). The flow crossed the open-closed field line boundary at 77° MLAT, and qualifies for an ionospheric signature of magnetopause reconnection burstjets. The flow direction was nearly parallel to the RKN radar beams, and therefore the RKN LOS measurements in Figure ~~4a~~ 5a approximated to the 2-d flow speed. The flow eastern boundary can be identified as where the velocity dropped from red/orange to blue (dashed magenta line). Determining the flow western boundary requires more measurements of the background convection velocity, which is beyond the RKN FOV. But we infer that the western boundary did not extend more than 1.5 h westward beyond the RKN FOV because the PGR and INV echoes there showed weakly poleward and equatorward LOS speeds around the open-closed field line boundary. The CLY radar data further indicated that the anti-sunward flow had started to rotate westward immediately beyond the RKN FOV. This is because the CLY LOS velocities measured between the RKN and INV radar FOVs were larger for more east-west oriented beams (appearing as yellow color) than for more north-south oriented beams (green color). The rotation likely corresponds to the vortex at the flow western boundary as sketched in *Oksavik et al.* [2004].

The more precise location of the western boundary can be retrieved from the SECS velocities in Figure ~~4b~~ 5b and the SHF velocities in Figure ~~4c~~5c. The SECS velocities present a flow channel very similar to that in Figure ~~4a~~5a, while the flow channel in the SHF velocities was more azimuthally-aligned than in Figures ~~4a~~5a-b.

The determined flow extent agrees with the extent of the cusp in Figure ~~4d~~5d. The high spectral widths associated with the cusp were located at the western half of the RKN FOV. They extended westward beyond the RKN FOV into CLY far range gates, where they dropped from red to green color. This is consistent with the inferred location and extent of the anti-sunward flow.

The flow of our interest just emerged from a weak background at the time when the THEMIS satellites crossed the magnetopause (Figure 5~~4~~e). This implies that the related reconnection ~~burst~~ just ~~initiated~~ activated at the studied local time. The flow ~~and the reconnection burst remained with a roughly~~spread azimuthally until 1833 UT when it stabilized. ~~steady and localized extent after~~

formation. We quantify the stabilized -flow extent and the reconnection electric field extent (Figure 5f) in a similar way as Figure 2f and Figure 3g. half width at half maximum (HWHM) of the flow using the RKN LOS velocity profile at 0830 UT (Figure 4f), and the HWHM was 10° MLON and 220 km. The FWHM of the flow is determined to be 432 and 336 km based on the SECS and RKN LOS data respectivelyusing the SECS velocities, and the FWHM was 26° MLON and 572 km. While the reconnection electric field had data gaps due to the limited coverage and backscatter availability at near range gate, it implies a western boundary of FWHM consistent with the flow slightly poleward of it. This is also the western boundary of non-zero reconnection rates considering the 15-mV/m uncertainty. The eastern boundary extended beyond RKN FOV. Such anThe FWHM of the SECS flow profile corresponds to ~45 Re in the equatorial plane.

The fact that the fast anti-sunward flow had a limited azimuthal extent around magnetic noon implies that the corresponding magnetopause reconnection burst should span over a limited local time range around the noon. This is consistent with the THEMIS satellite observation in Section 3.2.1, where reconnection was active at Y = 0.7 (THA) and 0.2 Re (THE). Projecting THA and THE locations to the ionosphere reveals that both satellite footprints were located within the flow longitudes. Therefore the reconnection at the two satellites was part of the same reconnection burst around the subsolar point of the magnetopause. (The THE footprint was equatorward of THA because the X location of THE was closer to the Earth than THA. The magnetopause was expanding and it swept across THE and then THA.) The reconnection further extended azimuthally beyond the two satellite locations, reaching a full length of ~45 Re.

3.3. Spatially continuous and extended reconnection active at both satellites

3.3.1. In-situ satellite measurements

On Apr 29, 2015, under a prolonged and steady southward IMF (Figure ~~5a~~6a), THA and THE crossed the magnetopause successively with a time separation of ~30 min. The locations of the crossings were separated by 0.1-0.2 Re in the Y direction (Figure ~~5b~~6b). The satellites passed from the magnetosphere into the magnetosheath, and the magnetic field data suggest that the satellites crossed the current layer multiple times before completely entering the magnetosheath (Figures 6i-r). We therefore only display the magnetic field and the plasma velocity in the GSM coordinates. Both satellites detected multiple flow jets, all agreeing with the Walen prediction with $\Delta V^* > 0.5$. For example, the jet at 1849-1850 UT measured by THA had a speed with 80% of and angle with 9° from the Walen prediction, and the jet at 1920-1922 UT by THE had a speed with 83% of and an angle with 1° from the Walen prediction. The ion distributions at THA and THE exhibit clear D-shaped distributions. ~~Such observations suggest that reconnection was active at the THA and THE local times.~~

3.3.2. Ground radar measurements

In the ionosphere, the radars detected a fast anti-sunward flow as an ionospheric signature of the magnetopause reconnection ~~burst~~ jet (Figures ~~6a~~7a-c). ~~The flow velocity here had a large component along the looking directions of the INV and CLY radars, and we therefore focus on the LOS measurements of these two radars.~~ The flow had a broad azimuthal extent, as delineated by the dashed magenta lines (Figure ~~6a~~7a). A similar flow distribution is found in the SECS velocities (Figure ~~6b~~7b), and the SHF velocities (Figure ~~6c~~7c). The flow propagated into the polar cap as one undivided channel (as opposed to Section 3.1.2), implying that it was one flow structure at least to the resolution the radars can resolve. Corresponding to the broad extent of the flow, the cusp had a broad extent (Figure ~~6d~~7d). The cusp continuously spanned across the INV and RKN

FOVs and its western and eastern edges coincided with the western and eastern boundaries of the flow, supporting our delineation of the flow extent.

The wide flow channel in the ionosphere implies that the corresponding magnetopause reconnection jetburst should be wide in local time. Based on the flow distribution, we infer that much of the reconnection burst should be located on the pre-noon sector, except that the eastern edge can extend across the magnetic noon meridian to the early post-noon sector. This inference is again consistent with the inference from the THA and THE measurements that the reconnection burst extended at least over the satellite separation (Y = -0.2 (THA) and 0 Re (THE)). Note, however, that the distance between THA and THE only covered <2% of the reconnection burst extent determined from the ionosphere flow. While the satellite configuration and measurements here were similar to those in Section 3.2, the extent of reconnection bursts was fundamentally different. This suggests that it is difficult to obtain a reliable estimate of the reconnection burst extent without the support of 2-d measurements and that satellites alone also cannot differentiate spatially extended reconnection from spatially patchy reconnection.

The flow temporal evolution is shown in Figures 7e 6e-f, where the velocities are the northward component of the SECS data. An overall wide flow channel is seen during the time interval of our interest with the eastern and western boundaries located at ~12.0-12.5 and ~8.0-8.7 h MLT, respectively. But between the two satellite observations, the flow experienced an interesting variation. The velocity at 9.3-12.0 h MLT dropped by 100-200 m/s during 1902-1912 UT (red color turned orange, yellow, and then green), while the velocity at 8.6-9.3 h MLT did not change substantially. The velocity enhanced again from 1912 UT. The enhancement centered at 10.7 h MLT and spread azimuthally towards east and west. The enhancement spread by 0.7 h MLT over 14 min at its eastern end (marked by the dashed black line), suggesting a spreading speed of 275 m/s. The enhancement spread by 1.2 h MLT at its western end, suggesting a spreading speed of 471 m/s. It should be noted that the all three components of the IMF stayed steady for an extended time (Figure 8, discussed below in Section 4), and thus the evolution of the flow/reconnection was unlikely to be externally driven.are based on the LOS measurements from the CLY (Figure 6e) and INV (Figure 6f) radars. The velocities >-18° MLON are not useful and are shaded in grey. These measurements were from short range gates of the CLY radar, where the convection velocity is underestimated as the Doppler velocity is limited below the ion acoustic speed (~400 m/s) [*Haldoupis*, 1989; *Koustov et al*., 2005]. An overall wide flow channel is seen between ~-90° and -30° MLON for most of the studied time period, and in particular the flow azimuthal extent were nearly identical at the instances when THA and THE observed the reconnection. But between the two satellite observations, the flow experienced an interesting variation. The velocity at -74°–-30° MLON dropped by 100-200 m/s during 1900-1910 UT, while the velocity at -88°-74° MLON did not change substantially. The velocity enhanced again from 1910 UT. The enhancement first occurred at ~-60°–-40° MLON and then spread azimuthally towards east and west. The enhancement spread by 18° over 14 min at its eastern end (marked by the dashed magenta line), suggesting a spreading speed of 429 m/s. The spreading at the western end soon merged with the velocity enhancement at -88°-74° MLON, but a rough estimate suggests a speed of 444 km/s. It should be noted that the all three components of the IMF stayed steady for an extended time (Figure 7, discussed below in Section 3.4), and thus the evolution of the flow/reconnection was unlikely to be externally driven.

This sequence of changes gives an important implication that the spatially extended reconnection was a result of spreading of an initially patchy reconnection. If we map the spreading in the ionosphere to the magnetopause, the spreading occurred bi-directionally and at a speed of

15 and 26 km/s in the east and west directions ~~24 km/s in each direction~~ based on field-line mapping under the T89 model (the mapping factor was 55). ~~The spreading process persisted for 10-20 min.~~ Such an observation is similar to what has recently been reported by *Zou et al.* [2018], where the reconnection also spreads bi-directionally at a speed of a few tens of km/s. However, the spreading in *Zou et al.* [2018] occurs following a southward turning of the IMF, while the spreading here occurred without IMF variations. The mechanism of spreading is explained either as motion of the current carriers of the reconnecting current sheet or as propagation of the Alfven waves along the guide field [*Huba and Rudakov*, 2002; *Shay et al.* 2003; *Lapenta et al.*, 2006; *Nakamura et al.*, 2012; *Jain et al.*, 2013].

It should be noted that reconnection spreading can be a common process of reconnection that is not limited to extended reconnection. It also occurs for patchy reconnection as seen in Sections 3.1 and 3.2. The spreading speeds were similar across the three events but the duration of the spreading process was two to three times longer in the spatially extended than the spatially patchy reconnection events. For the extended reconnection, the spreading process persisted for 14 min expanding the extent by 5-6 Re.~~A careful examination of Figure 4d suggests that spreading may have also occurred for the spatially patchy reconnection (the eastern limit of the red/orange region spread from -36° to -29° MLON during 1828-1832 UT). The two reconnection spread at a similarly speed, but duration of the spreading process was two to three times longer in the spatially extended than the spatially patchy reconnection events.~~

Figure~~s~~ 7f~~6g-h~~ quantifies~~y~~ the~~-~~ extent of the flow and reconnection electric field~~FWHM of the fast anti-sunward flow around the time when THA and THE measured active reconnection~~. The ~~width~~ FWHM extent was 1320 km based on the SECS data. Despite the presence of the data gaps, the LOS measurements suggest a western and eastern boundary consistent with the SECS data.

The reconnection electric field had a similar FWHM to the flow although regions of non-zero reconnection rates again extended beyond the available coverage indicating an overall extent >4 h MLT~~can be obtained based on the LOS measurements, where we determine the HWHMs of the flow in the INV and CLY FOVs separately and add them together as the FWHM. The FWHM was 63° MLON and 1260 km when THA measured the reconnection, and was 62° MLON and 1240 km when THE measured the reconnection~~. The extent~~is~~ corresponds to a reconnection ~~burst~~ extent of ~11 Re. ~~Note that the determination of the HWHM inside the CLY FOV has taken into account a background convection of ~400 m/s. The background came from those plasmas moving azimuthally along the open-closed field line boundary but not crossing the boundary. The width can also be obtained based on the SECS measurements, which was 64° MLON and 1280 km when THA measured the reconnection, and 60° MLON and 1200 km when THE measured the reconnection. This is very close to the values derived from the LOS measurements.~~

~~3.~~4. Discussion~~IMF and solar wind conditions for spatially patchy and extended reconnection~~

The above events definitely show that the local time extent of magnetopause reconnection ~~bursts~~ can vary from a few to >10 Re. Here we investigate whether and how the extent may depend on the upstream driving conditions. Figure ~~7~~8 presents the IMF, the solar wind velocity, and the solar wind pressure taken from the OMNI data for the three events. The red vertical lines mark the times when the reconnection was measured. The three events occurred under similar IMF field strengths (5-6 nT), similar IMF Bz components (-2-3 nT), and similar dynamic pressures (1-2 nPa), implying that the different reconnection ~~burst~~ extents were unlikely due to these parameters. The solar wind speeds had a slight decreasing trend as the reconnection extent increased~~were also similar among the three events, the speed being slightly larger for the spatially patchy than extended reconnection~~.

This is different from *Milan et al.* [2016], who identified ~~the solar wind velocity as the controlling factor of reconnection burst extent, where~~ a large~~r~~ solar wind speed as a cause of~~s~~ a large~~r~~ reconnection ~~burst~~ extent. However, *Milan et al.* [2016] studied reconnection under very strong IMF driving conditions when |B| ~15 nT, while our events occurred under a more typical moderate driving (|B| ~5-6 nT).

The spatially patchy reconnection events had an IMF Bx of a larger magnitude than the extended reconnection event did (4 vs. 0 nT). The spatially patchy reconnection events also had an IMF By component of a smaller magnitude (2 vs. 5 nT, and therefore a clock angle closer to 180°), and with more variability on time scales of tens of minutes, than the extended reconnection event. The IMF Bx and By components are known to modify the magnetic shear across the magnetopause and to affect the occurrence location of reconnection. Studies have found that at dayside low latitude magnetopause small $|B_y|/|B_z|$ relates to anti-parallel and large $|B_y|/|B_z|$ to component reconnection [*Coleman et al.*, 2001; *Chisham et al.*, 2002; *Trattner et al.*, 2007]. Large $|B_x|/|B|$, i.e. cone angle, also favors formation of high-speed magnetosheath jets [*Archer and Horbury*, 2013; *Plaschke et al.*, 2013] of a few Re in scale size, resulting in a turbulent magnetosheath environment for reconnection to occur [*Coleman, and Freeman*, 2005]. The steady IMF condition may allow reconnection to spread across local times unperturbedly, eventually reaching a wide extent. Thus our preliminary analysis suggests that the reconnection ~~burst~~ extent may depend on the IMF orientation and steadiness, although whether and how they influence the extent needs to be further explored.

5~~4~~. Summary

We carefully investigate the local time extent of magnetopause reconnection ~~bursts~~ by comparing the measurements of reconnection jets by two THEMIS satellites and three ground radars. The radars identify signatures of reconnection bursts as fast ionospheric flows moving anti-sunward across the open-closed field line boundary. When reconnection is activejets are only observed at only one of the two satellite locations, only the ionosphere conjugate to this spacecraft shows a channel of fast anti-sunward flow. When reconnection jets are observed is active at both spacecraft and the spacecraft are separated by <1 Re, the ionosphere conjugate to both spacecraft shows a channel of fast anti-sunward flow. The fact that the satellite locations are mapped to the same flow channel suggests that the reconnection is continuous between the two satellites, and that it is appropriate to take the satellite separation as a lower limit estimate of the reconnection burst extent. Whether reconnection can still be regarded as continuous when the satellites are separated by a few or > 10 Re is questionable, and needs to be examined using conjunctions with a larger satellite separation than what have been presented here.

The reconnection burst extent is measured as the FWHM extent of the ionospheric flow. In the three conjunction events, the flows have an extentFWHM of 260200, 572432, and 12601320 km in the ionosphere, which corresponds to ~32, 54, and 11 Re at the magnetopause (under the T89 model) in the local time direction. The flow extent is confirmed to be related to reconnection of high reconnection electric field. The resultis provides strong observational evidence that magnetopause reconnection bursts can occur over a wide range of extents, from spatially patchy (a few Re) to spatially continuous and extended (>10 Re). Interestingly, the extended reconnection is seen to initiate from a patchy reconnection, where the reconnection grows by spreading across local time. The speed of spreading is 50 41 km/s summing the westward and eastward spreading motion, and the spreading process persists for 10-2014 min broadening the extent by 5-6 Re.

Based on the three events studied in this paper, The the reconnection burst extent may be affected by the IMF orientation and steadiness, although the mechanism is not clearly known. For the observed modest solar wind driving conditions~~ studied here~~, the spatially extended reconnection is suggested to occur~~s~~ under a smaller IMF Bx component, and a larger and steadier IMF By component than the spatially patchy reconnection. The IMF strength, the Bz component, and the solar wind velocity and pressure are about the same for the extended and the patchy reconnection. This finding, however, could be limited by the number of events under analysis, and further study is needed to achieve an understanding of how solar wind controls reconnection extent. Reconnection can vary with time, even under steady IMF driving conditions.

Acknowledgments. This research was supported by the NASA Living With a Star Jack Eddy Postdoctoral Fellowship Program, administered by UCAR's Cooperative Programs for the Advancement of Earth System Science (CPAESS), NASA grant NNX15AI62G, NSF grants PLR-1341359 and AGS-1451911, and AFOSR FA9550-15-1-0179 and FA9559-16-1-0364. The THEMIS mission is supported by NASA contract NAS5-02099. SuperDARN is a collection of radars funded by national scientific funding agencies. SuperDARN Canada is supported by the Canada Foundation for Innovation, the Canadian Space Agency, and the Province of Saskatchewan. We thank Tomoaki Hori for useful discussion on the SECS technique. Data products of the SuperDARN, THEMIS, and OMNI are available at http://vt.superdarn.org/, http://themis.ssl.berkeley.edu/index.shtml, and GSFC/SPDF OMNIWeb website.

Reference

Amm, O., Grocott, A., Lester, M. and Yeoman, T. K.: Local determination of ionospheric plasma convection from coherent scatter radar data using the SECS technique, J. Geophys. Res., 115, A03304, doi:10.1029/2009JA014832, 2010.

Alexeev, I. I., Sibeck, D. G., and Bobrovnikov, S. Y.: Concerning the location of magnetopause merging as a function of the magnetopause current strength, J. Geophys. Res., 103(A4), 6675–6684, doi:10.1029/97JA02863, 1998.

Angelopoulos, V.: The THEMIS mission, Space Sci. Rev., 141, 5–34, doi:10.1007/s11214-008-9336-1, 2008.

Archer, M. O. and Horbury, T. S.: Magnetosheath dynamic pressure enhancements: occurrence and typical properties, Ann. Geophys., 31, 319-331, https://doi.org/10.5194/angeo-31-319-2013, 2013.

Auster, H. U., et al.: The THEMIS fluxgate magnetometer, *Space Sci. Rev.*, **141**, 235–264, 2008.

Baker, K. B., Dudeney, J. R., Greenwald, R. A., Pinnock, M., Newell, P. T., Rodger, A. S., Mattin, N. , and Meng, C.-I.: HF radar signatures of the cusp and low-latitude boundary layer, J. Geophys. Res., 100(A5), 7671–7695, doi:10.1029/94JA01481, 1995.

Baker, K. B., Rodger, A. S., and Lu, G.: HF-radar observations of the dayside magnetic merging rate: A Geospace Environment Modeling boundary layer campaign study, J. Geophys. Res., 102(A5), 9603–9617, doi:10.1029/97JA00288, 1997.

Bobra, M. G., Petrinec, S. M., Fuselier, S. A., Claflin, E. S., and Spence, H. E.: On the solar wind control of cusp aurora during northward IMF, Geophys. Res. Lett., 31, L04805, doi:10.1029/2003GL018417, 2004.

Borovsky, J. E.: Physical improvements to the solar wind reconnection control function for the Earth's magnetosphere, J. Geophys. Res. Space Physics, 118, 2113–2121, doi:10.1002/jgra.50110, 2013.

Bristow, W. A., Hampton, D. L., and Otto, A.: High-spatial-resolution velocity measurements derived using Local Divergence-Free Fitting of SuperDARN observations, J. Geophys. Res. Space Physics, 121, 1349–1361, doi:10.1002/2015JA021862, 2016.

Chisham, G., Coleman, I. J., Freeman, M. P., Pinnock, M., and Lester, M.: Ionospheric signatures of split reconnection X-lines during conditions of IMF Bz < 0 and |By|/|Bz|: Evidence for the antiparallel merging hypothesis, J. Geophys. Res., 107(A10), 1323, doi:10.1029/2001JA009124, 2002.

Chisham, G., and Freeman, M. P.: A technique for accurately determining the cusp-region polar cap boundary using SuperDARN HF radar measurements, Ann. Geophys., 21, 983–996, 2003.

Chisham, G., Freeman, M. P., Coleman, I. J., Pinnock, M., Hairston, M. R., Lester, M., and Sofko, G.: Measuring the dayside reconnection rate during an interval of due northward interplanetary magnetic field, Ann. Geophys., 22, 4243–4258, 2004.

Chisham, G., and M. P. Freeman: An investigation of latitudinal transitions in the SuperDARN Doppler spectral width parameter at different magnetic local times, Ann. Geophys., 22, 1187–1202, 2004.

Chisham, G., Freeman, M. P., and Sotirelis, T.: A statistical comparison of SuperDARN spectral width boundaries and DMSP particle precipitation boundaries in the nightside ionosphere, Geophys. Res. Lett., 31, L02804, doi:10.1029/2003GL019074, 2004b.

Chisham, G., Freeman, M. P., Sotirelis, T., Greenwald, R. A., Lester, M., and Villain J.-P.: A statistical comparison of SuperDARN spectral width boundaries and DMSP particle precipitation boundaries in the morning sector ionosphere, Ann. Geophys., 23,733–743, 2005a.

Chisham, G., Freeman, M. P., Sotirelis, T., and Greenwald, R. A.: The accuracy of using the spectral width boundary measured in off-meridional SuperDARN HF radar beams as a proxy for the open-closed field line boundary, Ann. Geophys., 23, 2599–2604, 2005b.

Chisham, G., Freeman, M. P., Lam, M. M., Abel, G. A., Sotirelis, T., Greenwald, R. A., and Lester, M.: A statistical comparison of SuperDARN spectral width boundaries and DMSP particle precipitation boundaries in the afternoon sector ionosphere, Ann. Geophys., 23, 3645–3654, 2005c.

Chisham, G., et al.: Remote sensing of the spatial and temporal structure of magnetopause and magnetotail reconnection from the ionosphere, Rev. Geophys., 46, RG1004, doi:10.1029/2007RG000223, 2008.

Coleman, I. J., Chisham, G., Pinnock, M., and Freeman, M. P., An ionospheric convection signature of antiparallel reconnection, J. Geophys. Res., 106, 28,995–29,007, 2001.

Coleman, I. J., and Freeman, M. P.: Fractal reconnection structures on the magnetopause, Geophys. Res. Lett., 32, L03115, doi:10.1029/2004GL021779, 2005.

Cousins, E. D. P., and Shepherd, S. G.: A dynamical model of high‐latitude convection derived from SuperDARN plasma drift measurements, *J. Geophys. Res.*, 115, A12329, doi:10.1029/2010JA016017, 2010.

Crooker, N. U., Dayside merging and cusp geometry, J. Geophys. Res., 84(A3), 951–959, doi:10.1029/JA084iA03p00951, 1979.

Crooker, N. U., F. R. Toffoletto, and M. S. Gussenhoven, Opening the cusp, J. Geophys. Res., 96(A3), 3497–3503, doi: 10.1029/90JA02099, 1991.

Denig, W. F., Burke, W. J., Maynard, N. C., Rich, F. J., Jacobsen, B., Sandholt, P. E., Egeland, S., Leontjev, A., and Vorobjev, V. G.: Ionospheric signatures of dayside magnetopause transients: A case study using satellite and ground measurements, *J. Geophys.*

Res., **98**(A4), 5969–5980, doi:10.1029/92JA01541, 1993.

Dorelli, J. C., Bhattacharjee, A., and Raeder, J.: Separator reconnection at Earth's dayside magnetopause under generic northward interplanetary magnetic field conditions, J. Geophys. Res., 112, A02202, doi:10.1029/2006JA011877, 2007.

Dunlop, M. W., et al.: Magnetopause reconnection across wide local time, *Ann. Geophys.*, **29**, 1683–1697, doi:10.5194/angeo-29-1683-2011, 2011.

Elphic, R. C., Lockwood, M., Cowley, S. W. H., and Sandholt, P. E.: Flux transfer events at the magnetopause and in the ionosphere, Geophys. Res. Lett., 17, 2241, 1990.

Fasel, G. J. (1995), Dayside poleward moving auroral forms: A statistical study, *J. Geophys. Res.*, 100(A7), 11891–11905, doi: 10.1029/95JA00854.

Fear, R. C., Milan, S. E., Fazakerley, A. N., Lucek, E. A., Cowley, S. W. H., and Dandouras, I.: The azimuthal extent of three flux transfer events, Ann. Geophys., 26, 2353-2369, https://doi.org/10.5194/angeo-26-2353-2008, 2008.

Fear, R. C., Milan, S. E., Lucek, E. A., Cowley, S. W. H., and Fazakerley, A. N.: Mixed azimuthal scales of flux transfer events, in *The Cluster Active Archive – Studying the Earth's Space Plasma Environment*, Astrophys. Space Sci. Proc., edited by H. Laakso, M. Taylor, and C. P. Escoubet, pp. 389–398, Springer, Dordrecht, Netherlands, doi:10.1007/978-90-481-3499-1_27, 2010.

Freeman, M. P., G. Chisham, and I. J. Coleman (2007), Remote sensing of reconnection, in Reconnection of Magnetic Fields, edited by J. Birn and E. Priest, chap. 4.6, pp. 217–228, Cambridge Univ. Press, New York.

Fuselier, S. A., Frey, H. U., Trattner, K. J., Mende, S. B., and Burch, J. L.: Cusp aurora dependence on interplanetary magnetic field Bz, J. Geophys. Res., 107(A7), 1111, doi:10.1029/2001JA900165, 2002.

Fuselier, S. A., Mende, S. B., Moore, T. E., Frey, H. U., Petrinec, S. M., Claflin, E. S., and Collier, M. R.: Cusp dynamics and ionospheric outflow, in Magnetospheric Imaging—The Image Mission, edited by J. L. Burch, Space Sci. Rev., 109, 285, doi:10.1023/B:SPAC.0000007522.71147.b3, 2003.

Fuselier, S. A., Trattner, K. J., Petrinec, S. M., Owen, C. J., and Rème, H., Computing the reconnection rate at the Earth's magnetopause using two spacecraft observations, J. Geophys. Res., 110, A06212, doi:10.1029/2004JA010805, 2005.

Fuselier, S. A., Petrinec, S. M., and Trattner, K. J.: Antiparallel magnetic reconnection rates at the Earth's magnetopause, J. Geophys. Res., 115, A10207, doi:10.1029/2010JA015302, 2010.

Glocer, A., Dorelli, J., Toth, G., Komar, C. M., and Cassak, P. A.: Separator reconnection at the magnetopause for predominantly northward and southward IMF: Techniques and results, J. Geophys. Res. Space Physics, 121, 140–156, doi:10.1002/2015JA021417, 2016.

Goertz, C. K., Nielsen, E., Korth, A., Glassmeier, K. H., Haldoupis, C., Hoeg, P., and Hayward, D.: Observations of a possible ground signature of flux transfer events, J. Geophys. Res., 90(A5), 4069–4078, doi:10.1029/JA090iA05p04069, 1985.

Gonzalez, W. D., and Mozer, F. S.: A quantitative model for the potential resulting from reconnection with an arbitrary interplanetary magnetic field, J. Geophys. Res., 79(28), 4186–4194, doi:10.1029/JA079i028p04186, 1974.

Gosling, J. T., Thomsen, M. F., Bame, S. J., Onsager, T. G., and Russell, C. T.: The electron edge of low latitude boundary layer during accelerated flow events, Geophys. Res. Lett., 17, 1833–1836, doi:10.1029/GL017i011p01833, 1990b.

Greenwald, R. A., et al.: DARN/SuperDARN: A global view of the dynamics of high-latitude convection, Space Sci. Rev., 71, 761–796, 1995.

Haerendel, G., Paschmann, G., Sckopke, N., Rosenbauer, H., and Hedgecock, P. C., The frontside boundary layer of the magnetosphere and the problem of reconnection, J. Geophys. Res., 83(A7), 3195–3216, doi:10.1029/JA083iA07p03195, 1978.

~~Haldoupis, C., A review on radio studies of auroral E-region ionospheric irregularities, *Ann. Geophys.*, **7**, 239–258, 1989.~~

Hasegawa, H., et al., Decay of mesoscale flux transfer events during quasi‐continuous spatially extended reconnection at the magnetopause, Geophys. Res. Lett., 43, 4755–4762, doi:10.1002/2016GL069225, 2016.

Haynes, A. L., and Parnell, C. E., A method for finding three-dimensional magnetic skeletons, *Phys. Plasmas*, **17**, 092903, doi:10.1063/1.3467499, 2010.

~~Hesse, M., Kuznetsova, M., and Birn, J., Particle-in-cell simulations of three-dimensional collisionless magnetic reconnection, J. Geophys. Res., 106(A12), 29831–29841, doi:10.1029/2001JA000075, 2001.~~

Huba, J. D., and Rudakov, L. I.: Three-dimensional Hall magnetic reconnection, Phys. Plasmas, 9, 4435, 2002.

Hudson, P. D., Discontinuities in an anisotropic plasma and their identification in the solar wind, Planet. Space Sci., 18, 1611–1622, 1970.

Jain, N., Büchner, J., Dorfman, S., Ji, H., and Sharma, A. S.: Current disruption and its spreading in collisionless magnetic reconnection, Phys. Plasmas 20, 112101, 2013.

Komar, C. M., Cassak, P. A., Dorelli, J. C., Glocer, A., and Kuznetsova, M. M., Tracing magnetic separators and their dependence on IMF clock angle in global magnetospheric simulations, J. Geophys. Res. Space Physics, 118, 4998–5007, doi:10.1002/jgra.50479, 2013.

~~Komar, C. M., Fermo, R. L., and Cassak, P. A.: Comparative analysis of dayside magnetic reconnection models in global magnetosphere simulations, *J. Geophys. Res. Space Physics*, 120, 276–294, doi:10.1002/2014JA020587, 2015.~~

~~Koustov, A. V., Danskin, D. W., Makarevitch, R. A., and Gorin, J. D.: On the relationship between the velocity of E-region HF echoes and E B plasma drift, *Ann. Geophys.*, **23**(2), pp. 371–378, 0992-7689, 2005.~~

Kuo, H., Russell, C. T., and Le, G., Statistical studies of flux transfer events, *J. Geophys. Res.*, 100(A3), 3513–3519, doi: 10.1029/94JA02498, 1995.

Laitinen, T. V., Janhunen, P., Pulkkinen, T. I., Palmroth, M., and Koskinen, H. E. J., On the characterization of magnetic reconnection in global MHD simulations, *Ann. Geophys.*, **24**, 3059–3069, 2006.

Laitinen, T. V., Palmroth, M., Pulkkinen, T. I., Janhunen, P., and Koskinen, H. E. J.: Continuous reconnection line and pressure-dependent energy conversion on the magnetopause in a global MHD model, *J. Geophys. Res.*, **112**, A11201, doi:10.1029/2007JA012352, 2007.

Lapenta, G., Krauss-Varban, D., Karimabadi, H., Huba, J. D., Rudakov, L. I., and Ricci, P.: Kinetic simulations of X-line expansion in 3D reconnection, Geophys. Res. Lett., 33, L10102, doi:10.1029/2005GL025124, 2006.

Lee, L. C., and Fu, Z. F., A theory of magnetic flux transfer at the earth's magnetopause, *Geophys. Res. Lett.*, **12**, 105, 1985.

Lockwood, M., Sandholt, P. E., and Cowley, S. W. H.: Dayside auroral activity and momentum transfer from the solar wind, *Geophys. Res. Lett.*, **16**, 33, 1989.

Lockwood, M., and Smith, M. F.: Low altitude signatures of the cusp and flux transfer events, *Geophys. Res. Lett.*, **16**, 879–882, 1989.

Lockwood, M., Cowley, S. W. H., Sandholt, P. E., and Lepping, R. P., The ionospheric signatures of flux transfer events and solar wind dynamic pressure changes, J. Geophys. Res., 95(A10), 17113–17135, doi:10.1029/JA095iA10p17113, 1990.

Lockwood, M., and Smith, M. F., Low and middle altitude cusp particle signatures for general magnetopause reconnection rate variations: 1. Theory, *J. Geophys. Res.*, 99(A5), 8531–8553, doi:10.1029/93JA03399, 1994.

Lockwood, M., et al: Co-ordinated Cluster and ground-based instrument observations of transient changes in the magnetopause boundary layer during an interval of predominantly northward IMF: Relation to reconnection pulses and FTE signatures, *Ann. Geophys.*, **19**, 1613–1640, doi:10.5194/angeo-19-1613-2001, 2001.

Luhmann, J. G., Walker, R. J., Russell, C. T., Crooker, N. U., Spreiter, J. R., and Stahara, S. S.: Patterns of potential magnetic field merging sites on the dayside magnetopause, *J. Geophys. Res.*, **89**, 1739–1742, doi:10.1029/JA089iA03p01739, 1984.

Lui, A. T. Y., and Sibeck, D. G.: Dayside auroral activities and their implications for impulsive entry processes in the dayside magnetosphere, *J. Atmos. Terr. Phys.*, **53**, 219, 1991.

McFadden, J. P., et al., The THEMIS ESA plasma instrument and in-flight calibration, *Space Sci. Rev.*, **141**, 277–302, 2008.

McWilliams, K. A., Yeoman, T. K., and Provan, G.: A statistical survey of dayside pulsed ionospheric flows as seen by the CUTLASS Finland HF radar, Ann. Geophys., 18, 445–453, doi:10.1007/s00585‐000‐0445‐8, 2000.

McWilliams, K. A., Yeoman, T.K., and Cowley, S.W.H.: Two-dimensional electric field measurements in the ionospheric footprint of a flux transfer event, Annales Geophysicae, 18, pp. 1584–1598, 2001a.

McWilliams, K. A., Yeoman, T.K., Sigwarth, J.B., Frank, L.A., and Brittnacher, M.:The dayside ultraviolet aurora and convection responses to a southward turning of the interplanetary magnetic field, Annales Geophysicae, 17, pp. 707–721, 2001b.

McWilliams, K. A., Yeoman, T.K., Sibeck, D.G., Milan, S.E., Sofko, G.J., Nagai, T., Mukai, T., Coleman, I.J., Hori, T., and Rich, F.J., Simultaneous observations of magnetopause flux transfer events and of their associated signatures at ionospheric altitudes, Annales Geophysicae, 22, pp. 2181–2199, 2004.

Milan, S. E., M. Lester, S. W. H. Cowley, and M. Brittnacher (2000), Convection and auroral response to a southward turning of the IMF: Polar UVI, CUTLASS, and IMAGE signatures of transient magnetic flux transfer at the magnetopause, J. Geophys. Res., 105(A7), 15741–15755, doi:10.1029/2000JA900022.

Milan, S. E., Imber, S. M., Carter, J. A., Walach, M.-T., and Hubert, B.: What controls the local time extent of flux transfer events?, J. Geophys. Res. Space Physics, 121, 1391–1401, doi:10.1002/2015JA022012, 2016.

Moen, J., Carlson, H. C., Milan, S. E., Shumilov, N., Lybekk, B., Sandholt, P. E., and Lester, M.: On the collocation between dayside auroral activity and coherent HF radar backscatter, Ann. Geophys., 18, 1531-1549, https://doi.org/10.1007/s00585-001-1531-2, 2000.

~~Moore, T. E., Fok, M. C., and Chandler, M. O.: The dayside reconnection X line, J. Geophys. Res., 107(A10), 1332, doi:10.1029/2002JA009381, 2002.~~

Nakamura, T. K. M., Nakamura, R., Alexandrova, A., Kubota, Y., and Nagai, T.: Hall magnetohydrodynamic effects for three-dimensional magnetic reconnection with finite width along the direction of the current, J. Geophys. Res., 117, A03220, doi:10.1029/2011JA017006, 2012.

Neudegg, D. A., Yeoman, T. K., Cowley, S. W. H., Provan, G., Haerendel, G., Baumjohann, W., Auster, U., Fornacon, K.-H., Georgescu, E., and Owen, C. J.: A flux transfer event observed at the magnetopause by the Equator-S spacecraft and in the ionosphere by the CUTLASS HF radar, Ann. Geophysicae, 17, 707, 1999.

Neudegg, D. A., et al., A survey of magnetopause FTEs and associated flow bursts in the polar ionosphere, *Ann. Geophys.*, **18**, 416, 2000.

Nishitani, N., Ogawa, T., Pinnock, M., Freeman, M. P., Dudeney, J. R., Villain, J.-P., Baker, K. B., Sato, N., Yamagishi, H., and Matsumoto, H.: A very large scale flow burst observed by the SuperDARN radars, J. Geophys. Res., 104(A10), 22469–22486, doi:10.1029/1999JA900241, 1999.

Newell, P. T., Meng, C.-I., Sibeck, D. G., and Lepping, R.: Some low-altitude cusp dependencies on the interplanetary magnetic field, J. Geophys. Res., 94(A7), 8921–8927, doi:10.1029/JA094iA07p08921, 1989.

Newell P. T., and Meng C.-I.: Ion acceleration at the equatorward edge of the cusp: Low-altitude observations of patchy merging, Geophys. Res. Lett., 18, 1829–1832, doi:10.1029/91GL02088, 1991.

Newell, P. T., and Meng, C.‐I : Ionospheric projections of magnetospheric regions under low and high solar wind conditions, J. Geophys. Res., 99, 273, 1994.

~~Newell, P. T., Wing, S. and Rich, F. J., Cusp for high and low merging rates, *J. Geophys. Res.*, 112, A09205, doi:10.1029/2007JA012353, 2007.~~

Newell, P. T., Sotirelis, T., Liou, K., Meng, C.‐I. and Rich, F. J., A nearly universal solar wind‐magnetosphere coupling function inferred from 10 magnetospheric state variables, J. Geophys. Res., 112, A01206, doi: 10.1029/2006JA012015, 2007b.

Tsyganenko, N. A., Modeling the Earth's magnetospheric magnetic field confined within a realistic magnetopause, J. Geophys. Res., 100(A4), 5599–5612, doi:10.1029/94JA03193, 1995.

Oksavik, K., Moen, J. and Carlson, H. C.: High-resolution observations of the small-scale flow pattern associated with a poleward moving auroral form in the cusp, *Geophys. Res. Lett.*, **31**, L11807, doi:10.1029/2004GL019838, 2004.

Oksavik, K., Moen, J., Carlson, H. C., Greenwald, R. A., Milan, S. E., Lester, M., Denig, W. F., and Barnes, R. J.: Multi-instrument mapping of the small-scale flow dynamics related to a cusp auroral transient, *Ann. Geophys.*, **23**, 2657–2670, 2005.

Paschmann, G., et al.: Plasma acceleration at the Earth's magnetopause: Evidence for magnetic reconnection, Nature, 282, 243, 1979.

Paschmann, G., et al.: The magnetopause for large magnetic shear: AMPTE/IRM observations, *J. Geophys. Res.*, **91**, 11,099, 1986.

Petrinec, S. M., and Fuselier, S. A.: On continuous versus discontinuous neutral lines at the dayside magnetopause for southward interplanetary magnetic field, Geophys. Res. Lett., 30(10), 1519, doi:10.1029/2002GL016565, 2003.

Phan, T. D., and Paschmann, G.: Low‐latitude dayside magnetopause and boundary layer for high magnetic shear: 1. Structure and motion, J. Geophys. Res., 101, 7801–7815, doi:10.1029/95JA03752, 1996.

Phan, T.-D., et al.: Extended magnetic reconnection at the Earth's magnetopause from detection of bi-directional jets, *Nature*, **404**, 848, 2000.

Phan, T.D., Freeman, M.P., Kistler, L.M. et al, Evidence for an extended reconnection line at the dayside magnetopause, Earth Planet Sp 53: 619. https://doi.org/10.1186/BF03353281, 2000.

Phan, T., et al.: Simultaneous Cluster and IMAGE observations of cusp reconnection and auroral proton spot for northward IMF, Geophys. Res. Lett., 30(10), 1509, doi:10.1029/2003GL016885, 2003.

Phan, T. D., Hasegawa, H., Fujimoto, M., Oieroset, M., Mukai, T., Lin, R. P., and Paterson, W. R.: Simultaneous Geotail and Wind observations of reconnection at the subsolar and tail flank magnetopause, Geophys. Res. Lett., 33, L09104,doi:10.1029/2006GL025756, 2006.

Phan, T. D., Paschmann, G., Gosling, J. T., Oieroset, M., Fujimoto, M., Drake, J. F., and Angelopoulos, V.: The dependence of magnetic reconnection on plasma β and magnetic shear: Evidence from magnetopause observations, Geophys. Res. Lett., 40, 11–16, doi:10.1029/2012GL054528, 2013.

Pinnock, M., Rodger, A. S., Dudeney, J. R., Baker, K. B., Newell, P. T., Greenwald, R. A., and Greenspan, M. E.: Observations of an enhanced convection channel in the cusp ionosphere, J. Geophys. Res., 98, 3767–3776, 1993.

Pinnock, M., Rodger, A. S., Dudeney, J. R., Rich, F., and Baker, K. B.: High spatial and temporal resolution observations of the ionospheric cusps, *Ann. Geophys.*, **13**, 919–925, 1995.

Pinnock, M & Rodger, A., On determining the noon polar cap boundary from SuperDARN HF radar backscatter characteristics. Annales Geophysicae. 18. 10.1007/s00585-001-1523-2, 2001.

Pinnock, M., Chisham, G., Coleman, I. J., Freeman, M. P., Hairston, M., and Villain, J.-P.: The location and rate of dayside reconnection during an interval of southward interplanetary magnetic field, Ann. Geophys., 21, 1467–1482, 2003.

Plaschke F, Hietala H., Angelopoulos V.: Anti-sunward high-speed jets in the subsolar magnetosheath. Ann. Geophys. 2013;31:1877–1889. doi:10.5194/angeo-31-1877-2013, 2013.

Ponomarenko, P. V., Waters, C. L., and Menk, F. W.: Factors determining spectral width of HF echoes from high latitudes, Ann. Geophys., 25, 675-687, https://doi.org/10.5194/angeo-25-675-2007, 2007.

Provan, G. & Yeoman, T.K.: Statistical observations of the MLT, latitude and size of pulsed ionospheric flows with the CUTLASS Finland radar, Annales Geophysicae, 17: 855. https://doi.org/10.1007/s00585-999-0855-1, 1999.

Provan, G., Yeoman, T. K., and Milan, S. E., CUTLASS Finland radar observations of the ionospheric signatures of flux transfer events and the resulting plasma flows, *Ann. Geophys.*, **16**, 1411–1422, 1998.

Ruohoniemi, J. M., Greenwald, R. A., Baker, K. B., Villain, J.-P., Hanuise, C., and Kelly, J.: Mapping high-latitude plasma convection with coherent HF radars, J. Geophys. Res., 94(A10), 13463–13477, doi:10.1029/JA094iA10p13463, 1989.

Ruohoniemi, J. M., and Baker, K. B.: Large-scale imaging of high-latitude convection with Super Dual Auroral Radar Network HF radar observations, J. Geophys. Res., 103(A9), 20797–20811, doi:10.1029/98JA01288, 1998.

Russell, C. T., and Elphic, R. C.: ISEE observations of flux transfer events at the dayside magnetopause, Geophys. Res. Lett., 6(1), 33–36, doi:10.1029/GL006i001p00033, 1979.

Sandholt, P. E., Deehr, C. S., Egeland, A., Lybekk, B., Viereck, R., and Romick, G. J.: Signatures in the dayside aurora of plasma transfer from the magnetosheath, J. Geophys. Res., 91(A9), 10063–10079, doi:10.1029/JA091iA09p10063, 1986.

Sandholt, P. E., Lockwood, M., Oguti, T., Cowley, S. W. H., Freeman, K. S. C., Lybekk, B., Egeland, A., and Willis, D. M.: Midday auroral breakup events and related energy and momentum transfer from the magnetosheath, J. Geophys. Res., 95(A2), 1039–1060, doi:10.1029/JA095iA02p01039, 1990.

Sandholt, P. E., et al.: Cusp/cleft auroral activity in relation to solar wind dynamic pressure, interplanetary magnetic field B_z and B_y , J. Geophys. Res., 99(A9), 17323–17342, doi:10.1029/94JA00679, 1994.

Scholer, M.: Magnetic flux transfer at the magnetopause based on single x line bursty reconnection, *Geophys. Res. Lett.*, **15**, 291, 1988.

Scholer, M., Sidorenko, I., Jaroschek, C. H., Treumann, R. A., and Zeiler, A.: Onset of collisionless magnetic reconnection in thin current sheets: Three-dimensional particle simulations, *Phys. Plasmas*, **10**(9), 3521–3527, 2003.

Shay, M. A., Drake, J. F., Swisdak, M., Dorland, W., and Rogers, B. N.: Inherently three dimensional magnetic reconnection: A mechanism for bursty bulk flows? Geophys. Res. Lett., 30(6), 1345, doi:10.1029/2002GL016267, 2003.

Shepherd, L. S., and Cassak, P. A.: Guide field dependence of 3-D X-line spreading during collisionless magnetic reconnection, J. Geophys. Res., 117, A10101, doi:10.1029/2012JA017867, 2012.

Smith, M., Lockwood, F.M., Cowley, S.W.H.: The statistical cusp: a simple flux transfer event model, *Planet Space Sci.*, 1992

Sonnerup, B. U. Ö., and Cahill Jr., L. J.: Magnetopause structure and attitude from Explorer 12 observations, *J. Geophys. Res.*, **72**, 171, 1967.

Sonnerup, B. U.: Magnetopause reconnection rate, J. Geophys. Res., 79(10), 1546–1549, doi:10.1029/JA079i010p01546, 1974.

Southwood, D. J.: Theoretical aspects of ionosphere‐magnetosphere‐solar wind coupling, Adv. Space Res., 5(4), 7–14, doi:10.1016/0273‐1177(85)90110‐3, 1985.

Southwood, D. J.: The ionospheric signature of flux transfer events, *J. Geophys. Res.*, **92**, 3207, 1987.

~~Swisdak, M., and Drake, J. F.: Orientation of the reconnection X-line, Geophys. Res. Lett., 34, L11106, doi:10.1029/2007GL029815, 2007.~~

Southwood, D. J., Farrugia, C. J., and Saunders, M. A.: What are flux transfer events? *Planet. Space Sci.*, **36**, 503, 1988.

Thorolfsson, A., Cerisier, J.-C., Lockwood, M., Sandholt, P. E., Senior, C. and Lester, M.: Simultaneous optical and radar signatures of poleward-moving auroral forms, *Ann. Geophys.*, **18**, 1054, 2000.

Trattner, K. J., Fuselier, S. A., and Petrinec, S. M.: Location of the reconnection line for northward interplanetary magnetic field, J. Geophys. Res., 109, A03219, doi:10.1029/2003JA009975, 2004.

Trattner, K. J., Mulcock, J. S., Petrinec, S. M., and Fuselier, S. A.: Probing the boundary between antiparallel and component reconnection during southward interplanetary magnetic field conditions, *J. Geophys. Res.*, 112, A08210, doi:10.1029/2007JA012270, 2007.

Trattner, K. J., Fuselier, S. A., Petrinec, S. M., Yeoman, T. K., Escoubet, C. P., and Reme, H.: The reconnection sites of temporal cusp structures, J. Geophys. Res., 113, A07S14, doi:10.1029/2007JA012776, 2008.

Trattner, K. J., Burch, J. L., Ergun, R., Eriksson, S., Fuselier, S. A., Giles, B. L., … Wilder, F. D. :The MMS dayside magnetic reconnection locations during phase 1 and their relation to the predictions of the maximum magnetic shear model. Journal of Geophysical Research:

Space Physics, 122, 11,991–12,005. https://doi.org/10.1002/2017JA024488, 2017.

Trenchi, L., Marcucci, M. F., Pallocchia, G., Consolini, G., Bavassano Cattaneo, M. B., Di Lellis, A. M., Rème, H., Kistler, L., Carr, C. M., and Cao, J. B.: Occurrence of reconnection jets at the dayside magnetopause: Double star observations, J. Geophys. Res., 113, A07S10, doi:10.1029/2007JA012774, 2008.

Tsyganenko, N. A.: A magnetospheric magnetic field model with a warped tail current sheet, Planet. Space Sci., 87, 5, 1989

Tsyganenko, N. A.: Modeling the Earth's magnetospheric magnetic field confined within a realistic magnetopause, J. Geophys. Res., 100(A4), 5599–5612, doi:10.1029/94JA03193, 1995.

Tsyganenko, N. A.: A model of the magnetosphere with a dawn-dusk asymmetry, 1, Mathematical structure, J. Geophys. Res., 107(A8), doi:10.1029/2001JA000219, 2002a.

Tsyganenko, N. A.: A model of the near magnetosphere with a dawn-dusk asymmetry, 2, Parameterization and fitting to observations, J. Geophys. Res., 107(A8), doi:10.1029/2001JA000220, 2002b.

Walsh, B. M., Foster, J. C., Erickson, P. J., and Sibeck, D. G.: Simultaneous ground- and space-based observations of the plasmaspheric plume and reconnection, *Science*, **343**, 1122–1125, doi:10.1126/science.1247212, 2014a.

Walsh, B. M., Phan, T. D., Sibeck, D. G., and Souza, V. M.: The plasmaspheric plume and magnetopause reconnection, Geophys. Res. Lett., 41, 223–228, doi:10.1002/2013GL058802, 2014b.

Walsh, B. M., Komar, C. M., and Pfau-Kempf, Y.: Spacecraft measurements constraining the spatial extent of a magnetopause reconnection X line, Geophys. Res. Lett., 44, 3038–3046, doi:10.1002/2017GL073379, 2017.

Wang, Y., et al.: Initial results of high-latitude magnetopause and low-latitude flank flux transfer events from 3 years of Cluster observations, J. Geophys. Res., 110, A11221, doi:10.1029/2005JA011150, 2005.

Wang, J., et al., TC1 and Cluster observation of an FTE on 4 January 2005: A close conjunction, Geophys. Res. Lett., 34, L03106, doi:10.1029/2006GL028241, 2007.

Wild, J. A., Cowley, S. W. H., Davies, J. A., Khan, H., Lester, M., Milan, S. E., Provan, G., Yeoman, T. K., Balogh, A., Dunlop, M. W., Fornacon, K.-H., and Georgescu, E.: First simultaneous observations of flux transfer events at the high-latitude magnetopause by the Cluster spacecraft and pulsed radar signatures in the conjugate ionosphere by the CUTLASS and EISCAT radars, Ann. Geophys., 19, 1491–1508, 2001.

Wild, J. A., Milan, S. E., Davies, J. A., Cowley, S. W. H., Carr, C. M., and Balogh, A.: Double Star, Cluster, and groundbased observations of magnetic reconnection during an interval of duskward oriented IMF: preliminary results, Ann. Geophys., 23, 2903–2907, 2005.

Wild, J. A., Milan, S. E., Davies, J. A., Dunlop, M. W., Wright, D. M., Carr, C. M., Balogh, A., Reme, H., Fazakerley, A. N., ` and Marchaudon, A.: On the location of dayside magnetic reconnection during an interval of duskward oriented IMF, Ann. Geophys., 25, 219–238, 2007.

Zhang, Q.-H., et al.: Simultaneous tracking of reconnected flux tubes: Cluster and conjugate SuperDARN observations on 1 April 2004, *Ann. Geophys.*, **26**, 1545–1557, doi:10.5194/angeo-26-1545-2008, 2008.

Zou, Y., Walsh, B. M., Nishimura, Y., Angelopoulos, V., Ruohoniemi, J. M., McWilliams, K. A., *&* Nishitani, N. Spreading speed of magnetopause reconnection X-lines using ground-satellite coordination. Geophysical Research Letters, 45. https://doi.org/10.1002/2017GL075765, 2018.

Figure 1a: OMNI IMF condition on Feb 2, 2013. Figure 1b: THE and THA locations projected to the GSM X-Y plane. The inner curve marks the magnetopause and the outer curve marks the bow shock.

Figure 2a: SuperDARN LOS speeds (color tiles) and merged velocity vectors (color arrows) in the Altitude adjusted corrected geomagnetic (*AACGM*) coordinates. The FOVs of the RKN, INV, and CLY radars are outlined with the black dashed lines. The colors of the tiles indicate the LOS speeds away from the radar. The colors and the lengths of the arrows indicate the merged velocity magnitudes and the arrow directions indicate the velocity directions. Red and anti-sunward directed flows are the ionospheric signature of magnetopause reconnection. The dashed magenta lines mark the flow western and eastern boundaries. The open-closed field line boundary was delineated by the dashed black curve marked by the "OCB" marker. The satellite footprints under the T89 are shown as the THE and THA marker. Figure 2b: Similar to Figure 2a but showing SECS velocity vectors (color arrows). Figure 2c: Similar to Figure 2a but showing SHF velocity vectors (color arrows). Figure 2d: SuperDARN spectral width measurements (color tiles). The red contour marks localized enhanced soft electron precipitation. Figure 2e: Time evolution of the northward component of SECS velocities along 79° MLAT~~INV LOS velocities along 80° MLAT~~. ~~The velocities are color coded in the same way as Figure 2a.~~ Figure 2f: Profile of convection velocities along 79° MLAT at 1929 UT as a function of the distance from magnetic noon. ~~Longitudinal profile of convection velocities along 80° MLAT at 1925 UT. The profile is also shown as a function of the distance measured azimuthally from 0° MLON.~~ The profile in black is based on the LOS measurements and the profile in red is the northward component of the SECS velocities. The FWHM is determined based on each profile. Figures 2g-j: THE measured magnetic field (0.25 s resolution), ion energy flux (3 s), ion density (3 s), and ion velocity (3 s). The ion measurements were taken from ground ESA moments. The magnetic field and the ion velocity components are displayed in the LMN boundary normal coordinate system. The magnetopause crossing is shaded in pink. Figure 2k: THE ion distribution function on the bulk velocity-magnetic field plane. The small black line indicates the direction and the bulk velocity of the distributions. Figures 2l-p: THA measurements in the same format as in Figures 2g-k. Figures 2q-z: THA and THE measurements during a subsequent magnetopause crossing shown in the same format as in Figures 2g-p.

Figures 3a-c: Snapshots of spectral width measurements around the space-ground conjunction time and longitude. The open-closed field line boundary is drawn as the dashed black line. Figures 3d-f: time series of the spectral width measurements along INV beams 4, 7, and 10, as a function of latitude, from which the motion of the open-closed field line boundary can be derived. Figure 3g: the electric field along the open-closed field line boundary in the frame of boundary (solid) and in the rest frame (dashed) following Pinnock et al. [2003], Freeman et al. [2007], Chisham et al. [2008]. The former is the reconnection electric field.

Figure 4~~3~~: OMNI IMF condition and THEMIS satellite locations on Apr 19, 2015 in a similar format to Figure 1.

Figure 5~~4~~. THEMIS and SuperDARN measurements of reconnection bursts on Apr 19, 2015 in a similar format to Figure 2. The velocity time evolution in Figure 5~~4~~e and the velocity profile in Figure 5~~4~~f are taken along ~~79~~ 78° MLAT.

Figure 6~~5~~. OMNI IMF condition and THEMIS satellite locations on Apr 29, 2015 in a similar format to Figure 1.

Figure 7. THEMIS and SuperDARN measurements of reconnection bursts on Apr 29, 2015 in a similar format to Figure 2. The velocity time evolution in Figure 7e and the velocity profile in Figure 7f are taken along 79° MLAT. The two branches of the LOS velocity profile in Figure 7f are based on INV and RKN LOS data. The magnetic field and plasma velocities measured by spacecraft are displayed in the GSM coordinates.

~~Figures 6a-d: SuperDARN measurements of reconnection bursts on Apr 29, 2015 in a similar~~

~~format to Figures 2a-d except that in Figure 6a the color of the CLY color tiles represent LOS speeds towards the radar as here LOS speeds towards the CLY radar project to the anti-sunward direction. Figures 6e-f: Time evolution of LOS velocities along 80° MLAT from the INV and CLY radars. The velocity measurements in the shaded region are backscatters from the E-region ionosphere and thus underestimate the convection speed. The flow channel spread azimuthally before reaching an extended extent, and the time-dependent locations of its western and eastern boundaries are marked by the dashed magenta lines. Figures 6g-h: Longitudinal profiles of the LOS and the poleward SECS velocities along 80° MLAT when THA and THE observed reconnection. Figures 6i-r: THEMIS measurements of reconnection bursts in a similar format to Figures 2g-p, but the magnetic field and plasma velocities are displayed in the GSM coordinates.~~

Figure 8~~7~~. Comparison of the IMF and solar wind driving conditions between the reconnection events on Feb 2, 2013, Apr 19, 2015, and Apr 29, 2015. From top to bottom: IMF in GSM coordinates, IMF clock angle, solar wind speed, and solar wind dynamic pressure. The red vertical lines mark the times of the satellite-ground conjunction.

Figure 1.

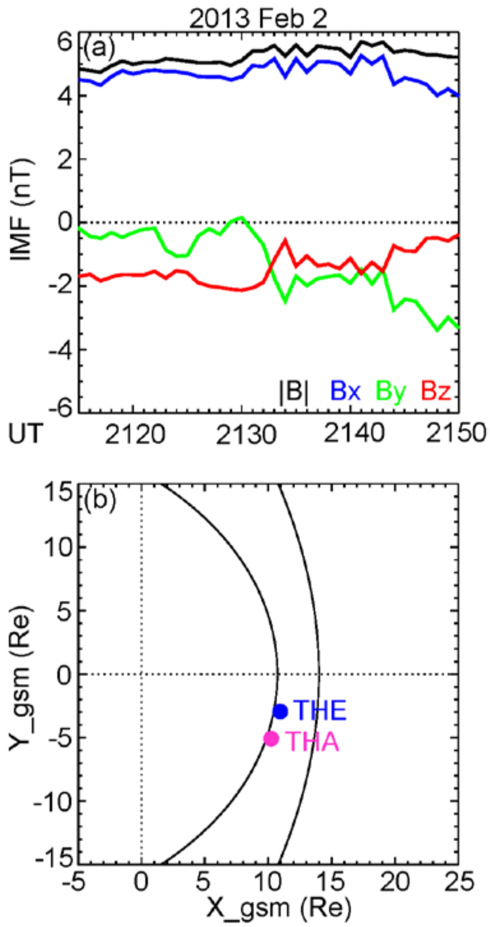
2013 Feb 2
(a)
IMF (nT)
|B| Bx By Bz
UT
2120
2130
2140
2150
(b)
Y_gsm (Re)
THE
THA
X_gsm (Re)

1222 Figure 2.

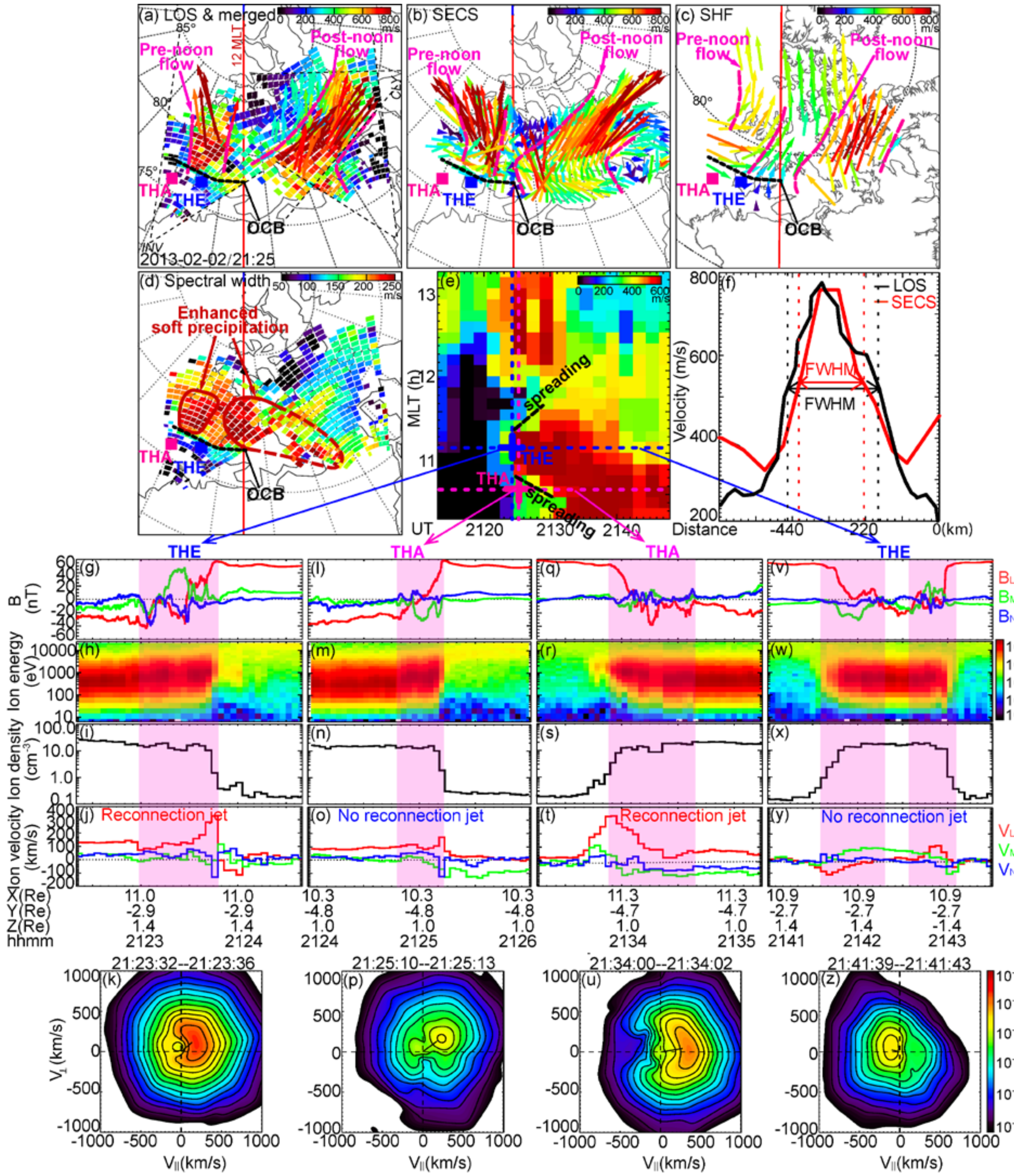

1223

1224

1225

1226

Figure 3.

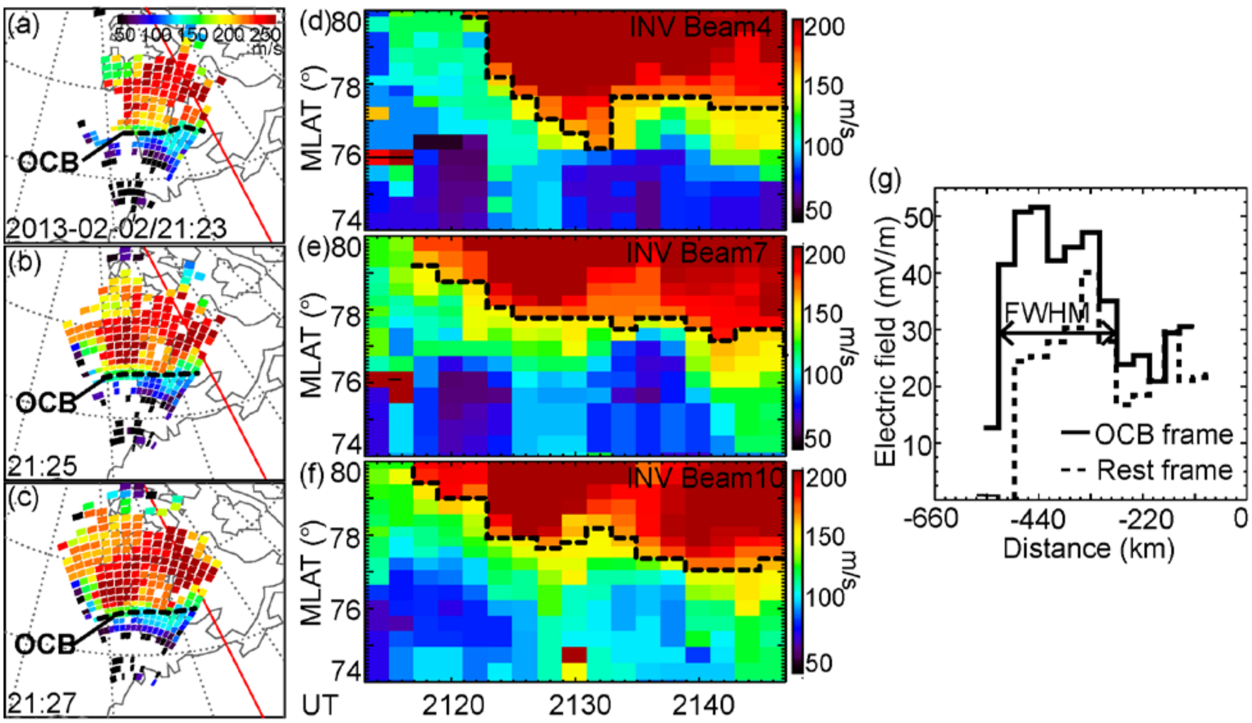
(a)
50 100 150 200 250
m/s
OCB
2013-02-02/21:23
(b)
OCB
21:25
(c)
OCB
21:27
(d)
INV Beam4
(e)
INV Beam7
(f)
INV Beam10
MLAT (°)
80
78
76
74
UT
2120
2130
2140
200
150
100
50
m/s
(g)
Electric field (mV/m)
50
40
30
20
10
FWHM
OCB frame
Rest frame
-660
-440
-220
0
Distance (km)

Figure 4.

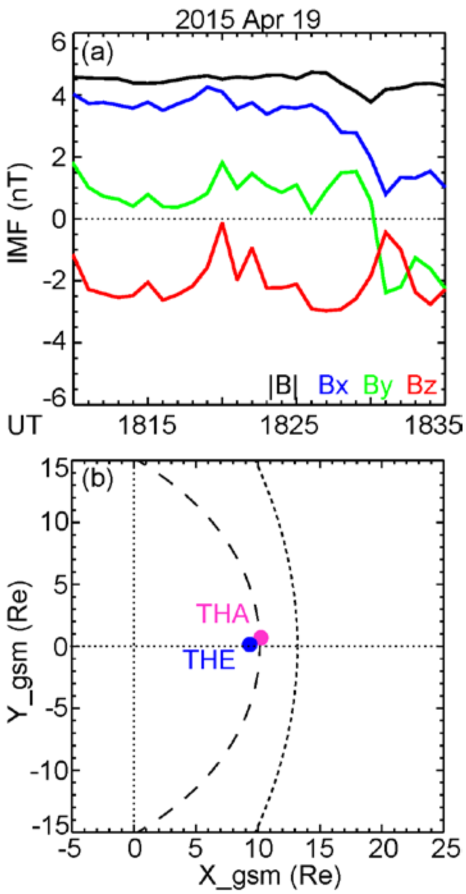
2015 Apr 19
(a)
IMF (nT)
|B| Bx By Bz
UT
1815
1825
1835
(b)
THA
THE
Y_gsm (Re)
X_gsm (Re)

1252 Figure 5.

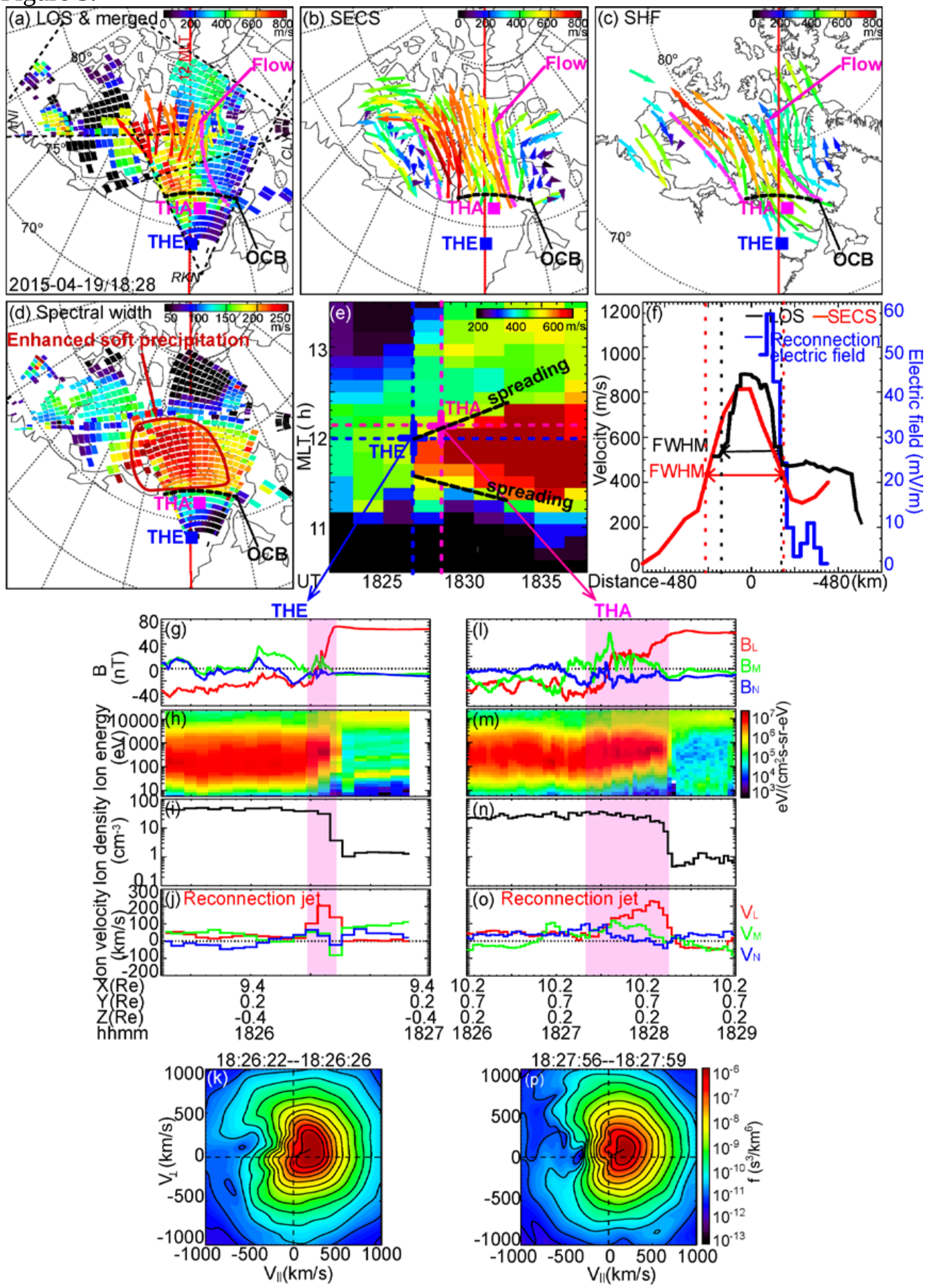

1253

Figure 6.

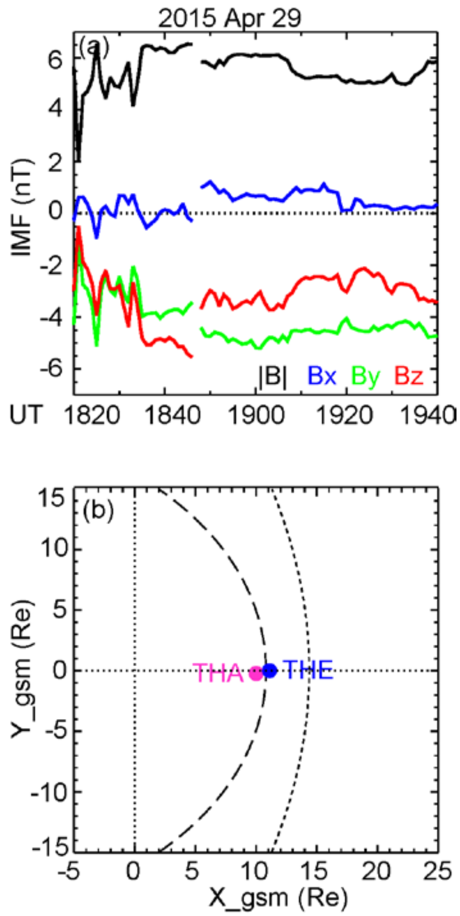

2015 Apr 29
(a)
IMF (nT)
6
4
2
0
-2
-4
-6
|B| Bx By Bz
UT 1820 1840 1900 1920 1940
(b)
15
10
5
0
-5
-10
-15
Y_gsm (Re)
THA
THE
-5 0 5 10 15 20 25
X_gsm (Re)

Figure 7.

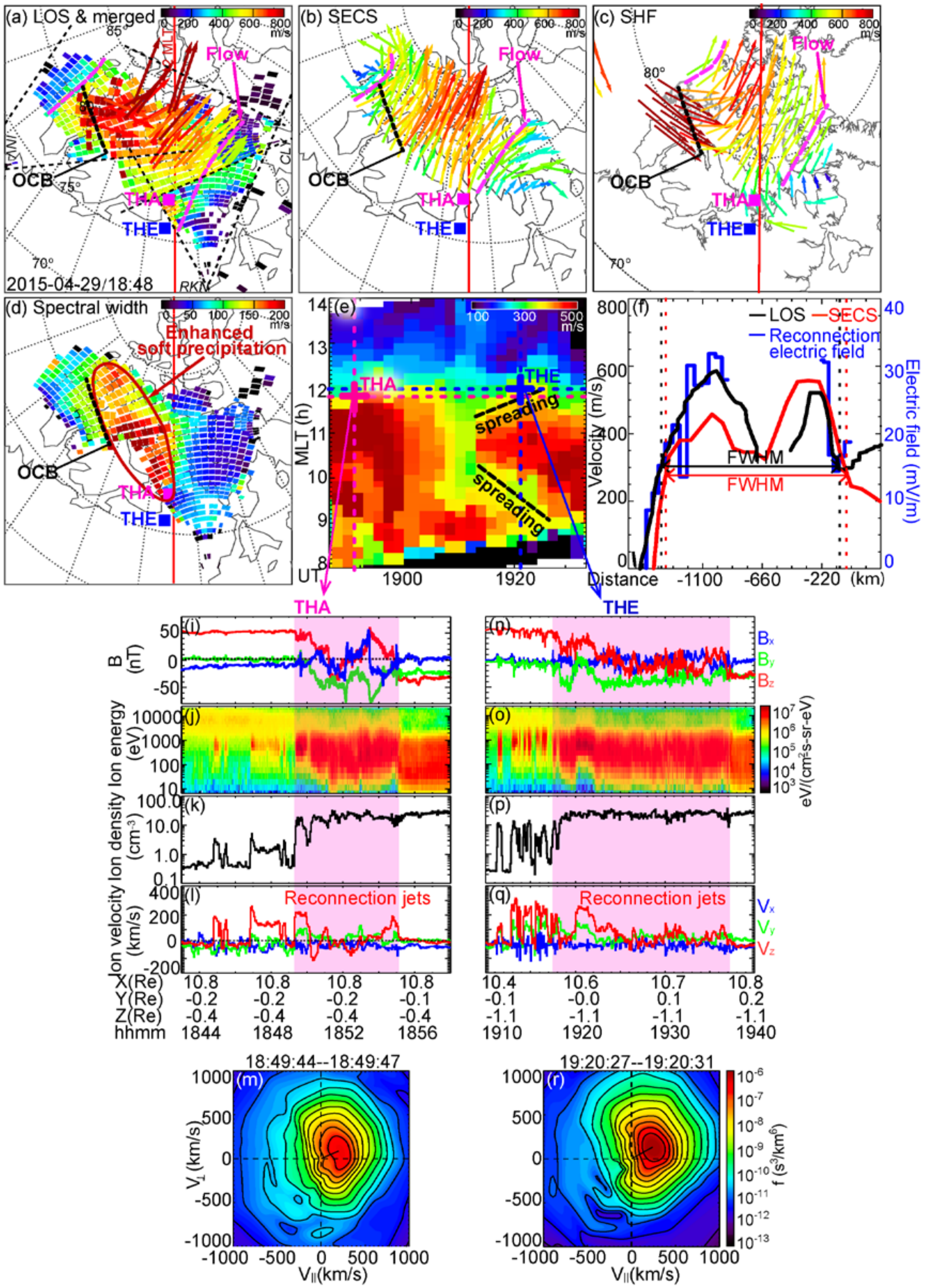

(a) LOS & merged
(b) SECS
(c) SHF
Flow
OCB
THA
THE
2015-04-29/18:48
(d) Spectral width
Enhanced soft precipitation
(e)
MLT (h)
spreading
UT
1900
1920
(f)
LOS
SECS
Reconnection electric field
Velocity (m/s)
Electric field (mV/m)
FWHM
Distance
-1100
-660
-220
(km)
(i)
(j)
(k)
(l)
(n)
(o)
(p)
(q)
B (nT)
Ion energy (eV)
Ion density (cm^-3)
Ion velocity (km/s)
eV/(cm^2-s-sr-eV)
Reconnection jets
X(Re)
Y(Re)
Z(Re)
hhmm
18:49:44--18:49:47
19:20:27--19:20:31
(m)
(r)
V⊥(km/s)
V||(km/s)
f (s^3/km^6)

Figure 8.

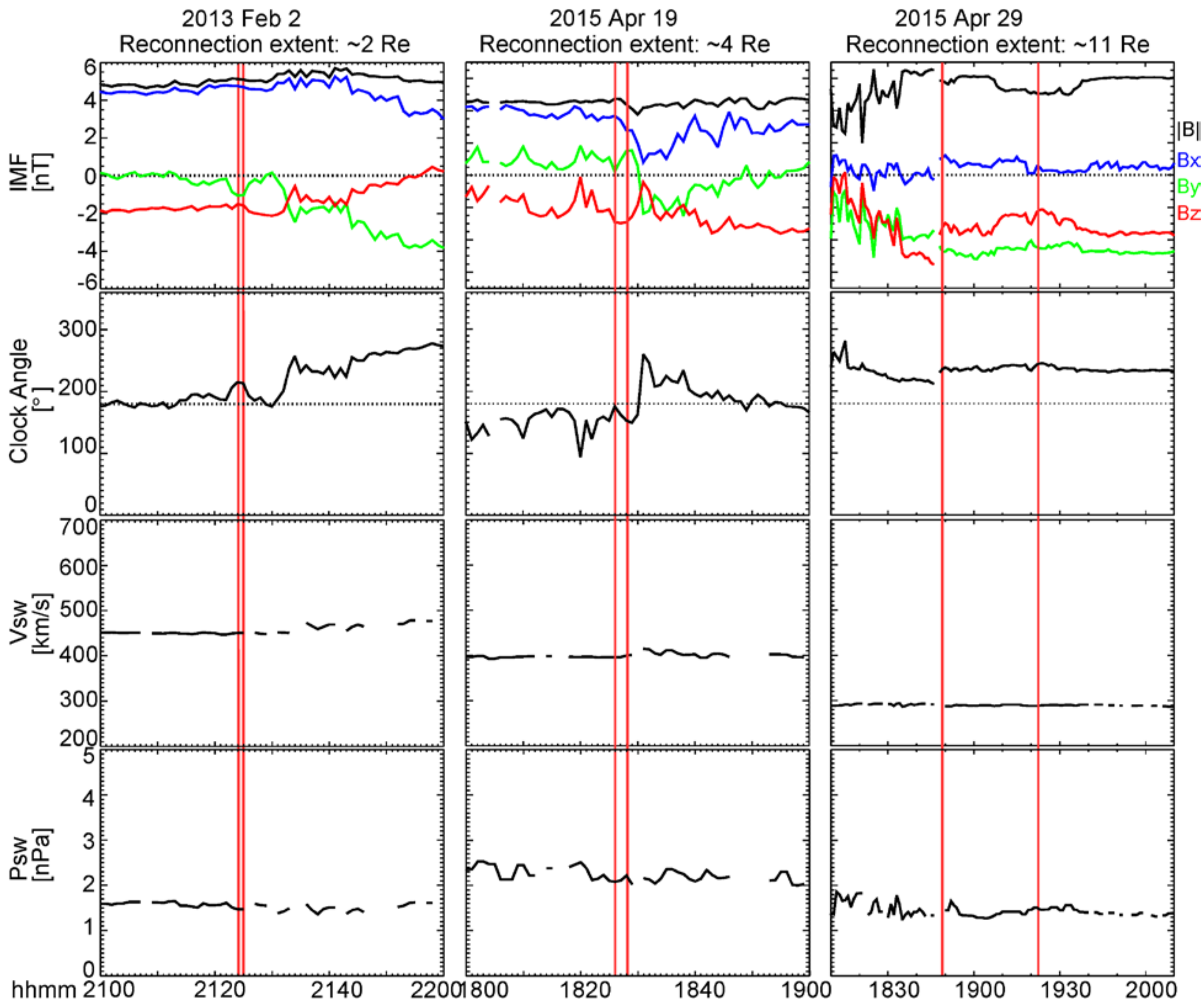

2013 Feb 2
Reconnection extent: ~2 Re
2015 Apr 19
Reconnection extent: ~4 Re
2015 Apr 29
Reconnection extent: ~11 Re
IMF [nT]
|B|
Bx
By
Bz
Clock Angle [°]
Vsw [km/s]
Psw [nPa]
hhmm 2100 2120 2140 2200
1800 1820 1840 1900
1830 1900 1930 2000